B Physics in CMS

Silvia Goy López (CIEMAT)

For the CMS collaboration

LHC2010, October 4th-9th 2010, Split

Outline and references

- **J//ψ** prompt and non-prompt cross sections in pp collisions at $\sqrt{s}$ = 7TeV (CMS PAS BPH-10-002)
- **Upsilon** production cross section in pp collisions at $\sqrt{s}$ = 7TeV (CMS PAS BPH-10-003)
- **Open beauty** production cross section with muons in pp collisions at $\sqrt{s}$ = 7TeV (CMS PAS BPH-10-007)
- **Inclusive b-jet** production in pp collisions at $\sqrt{s}$ = 7TeV (CMS PAS BPH-10-009)

The CMS detector

- CMS very well suited for b-physics due to excellent tracking and muon detectors
  - Pixel detector for precise reconstruction for secondary vertexes
  - Excellent tracking efficiency and resolution
  - Muon system with ability to trigger on low p_T muons

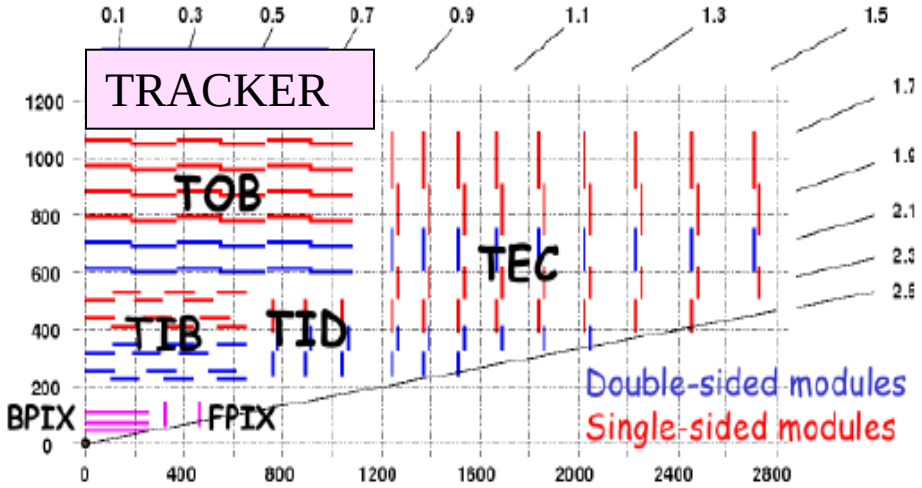

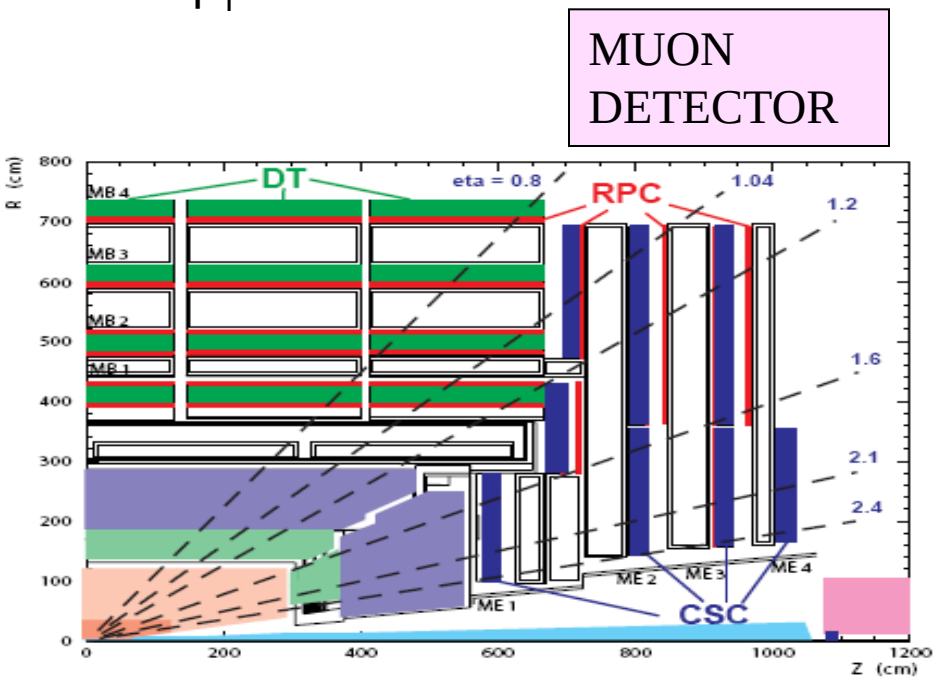

J/ψ and Υ cross sections

- Theoretical models do not simultaneously describe the cross-section and polarization measurements at Tevatron. New results from LHC at higher energies and wider rapidity ranges can help clarifying the quarkonium production mechanism
- Non-prompt charmonium production leads to a direct measurement of bb cross section. Measurements at LHC allow testing current theoretical models at high energy and help to validate QCD and PDFs
- J/ψ and Υ measurements are starting point for dimuon analysis in CMS

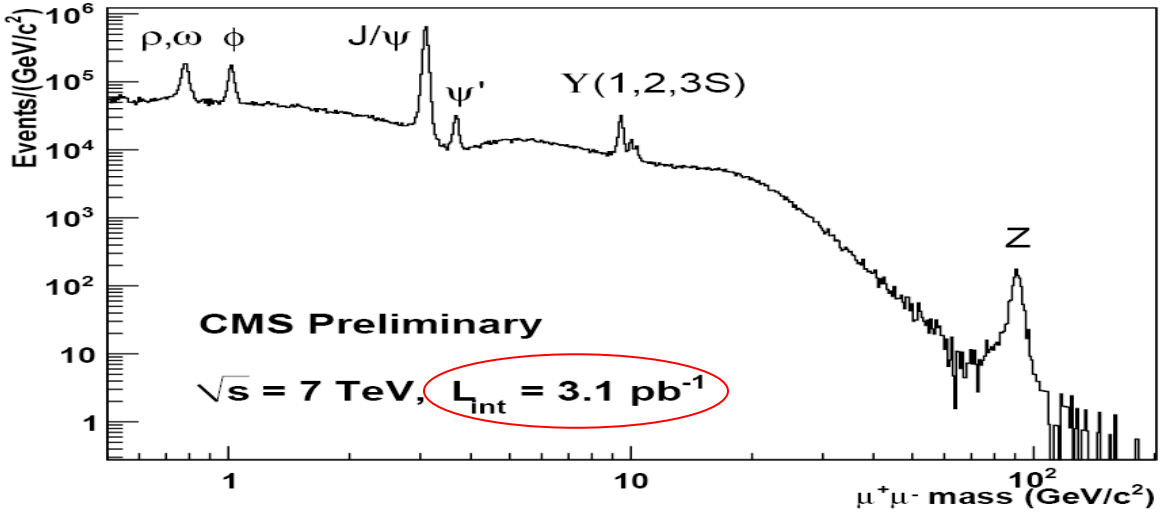

Inclusive J/ψ production cross section

$$\frac{d^2\sigma}{dp_T dy}(pp \to Q\bar{Q}X) \times \mathcal{B}(Q\bar{Q} \to \mu^+\mu^-) = \frac{N_{Q\bar{Q}}}{\int Ldt \cdot A \cdot \epsilon_{trigger} \cdot \epsilon_{reco} \cdot \Delta p_T \Delta y}$$

- Selection:
  - Opposite sign muons constrained to vertex (χ^2 cut) with $2.6<M(\mu^+\mu^-)<3.5$ GeV/c^2
  - Quality cuts: # hits, χ^2
  - Muon kinematic cuts

$$\begin{aligned} |\eta^\mu| &< 1.3 \quad p_T^\mu > 3.3 \text{ GeV}/c \\ 1.3 < |\eta^\mu| &< 2.2 \quad p^\mu > 2.9 \text{ GeV}/c \\ 2.2 < |\eta^\mu| &< 2.4 \quad p_T^\mu > 0.8 \text{ GeV}/c \end{aligned}$$

- Muon reconstruction and trigger efficiency computed from data using tag+probe method (plus MC correction)

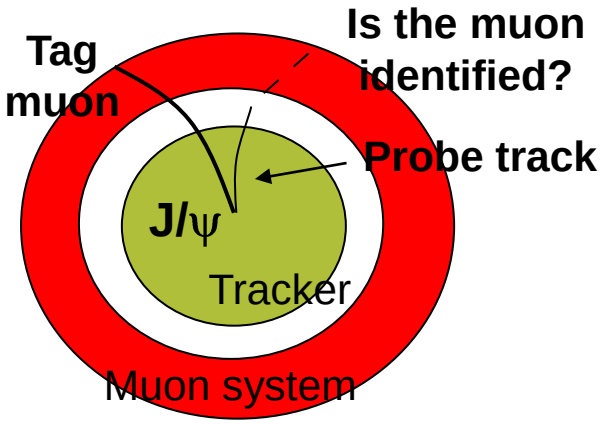

Inclusive J/ψ production cross section

$$\frac{d^2\sigma}{dp_T dy}(pp \to Q\bar{Q}X) \times \mathcal{B}(Q\bar{Q} \to \mu^+\mu^-) = \frac{N_{Q\bar{Q}}}{\int Ldt \cdot A \cdot \epsilon_{trigger} \cdot \epsilon_{reco} \cdot \Delta p_T \Delta y}$$

- Acceptance from MC simulation. Dependent on assumed polarization
  - Various polarization scenarios for prompt component
  - Non-prompt component modeled from b-factory experimental results.
- Yield: Cristal Ball plus exponential in p_T bins, in two rapidity ranges.
  - Central region better resolution and low background
  - End-cap region down to p_T~0

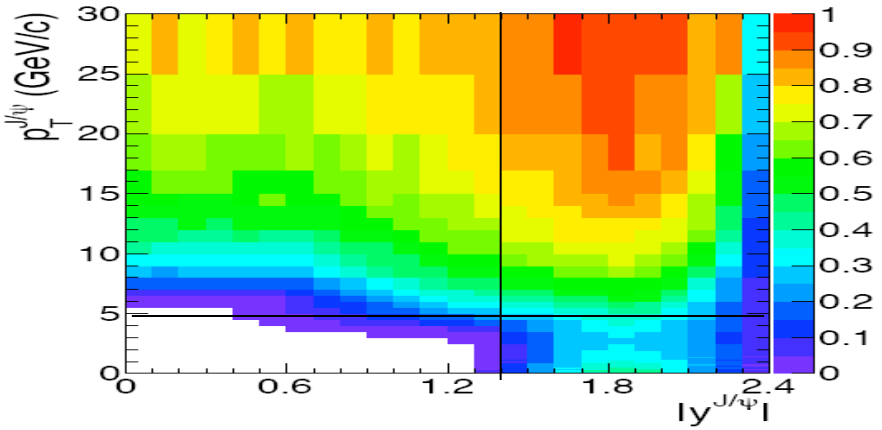

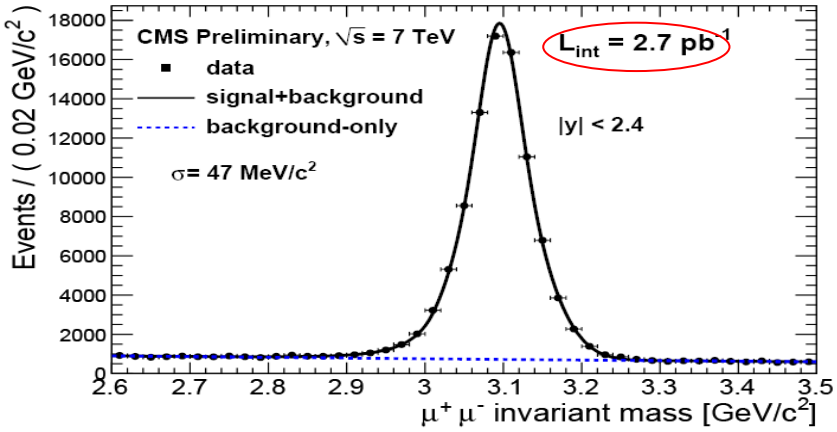

Inclusive J/ψ production cross section

- Results for 100 nb^{-1}
- Differential vs $p_T(J/\psi)$<30 GeV/c in two rapidity regions

- Main source of systematic uncertainty from muon efficiency. Will be reduced with additional data

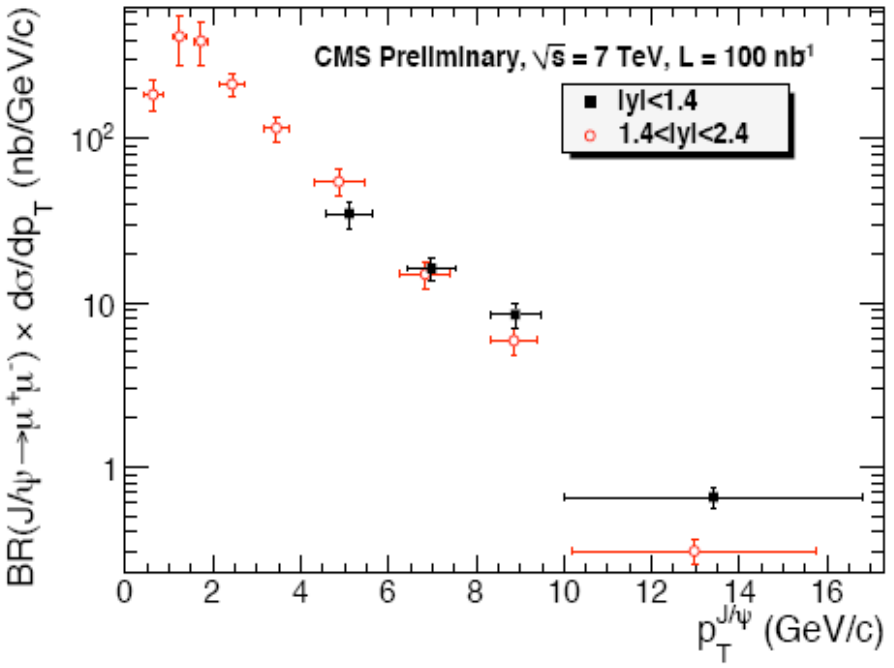

- Total cross section for inclusive J/ψ production 4< $p_T(J/\psi)$< 30 GeV/c, |y(J/ψ)|<2.4

$$BR(J/\psi \to \mu^+\mu^-) \cdot \sigma(pp \to J/\psi + X) = (289.1 \pm 16.7(\text{stat}) \pm 60.1(\text{syst}))\ \text{nb}$$

J/ψ prompt vs non-prompt

- For each candidate estimate B-hadron decay length = $l_{J/\psi}$ = $L_{xy} \cdot m_{J/\psi} / p_T$

Signed decay length of secondary vertexes

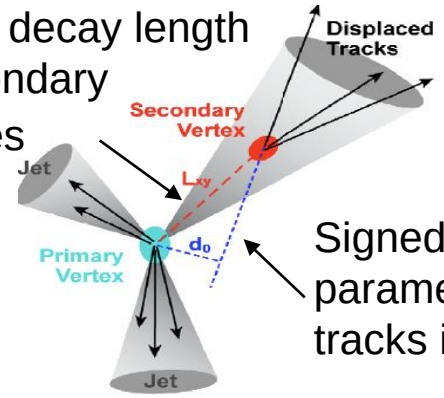

Signed impact parameter of tracks in the jet

- Fraction of J/ψ's from B-hadron decays obtained by ML fit to $F(l_{J/\psi}, M(\mu^+\mu^-))$ in p_T bins

$$F(\ell_{J/\psi}, m_{\mu\mu}) = f_{Sig} \cdot F_{Sig}(\ell_{J/\psi}) \cdot M_{Sig}(m_{\mu\mu}) + (1 - f_{Sig}) \cdot F_{Bkg}(\ell_{J/\psi}) \cdot M_{Bkg}(m_{\mu\mu})$$

$$F_{Sig}(\ell_{J/\psi}) = f_B \cdot F_B(\ell_{J/\psi}) + (1 - f_B) \cdot F_p(\ell_{J/\psi})$$

- Main source of systematic uncertainty from primary vertex estimation and resolution model for prompt component

J/ψ prompt vs non-prompt

2< p_T(J/ψ)<4 GeV/c, 1.4<|y|<2.4

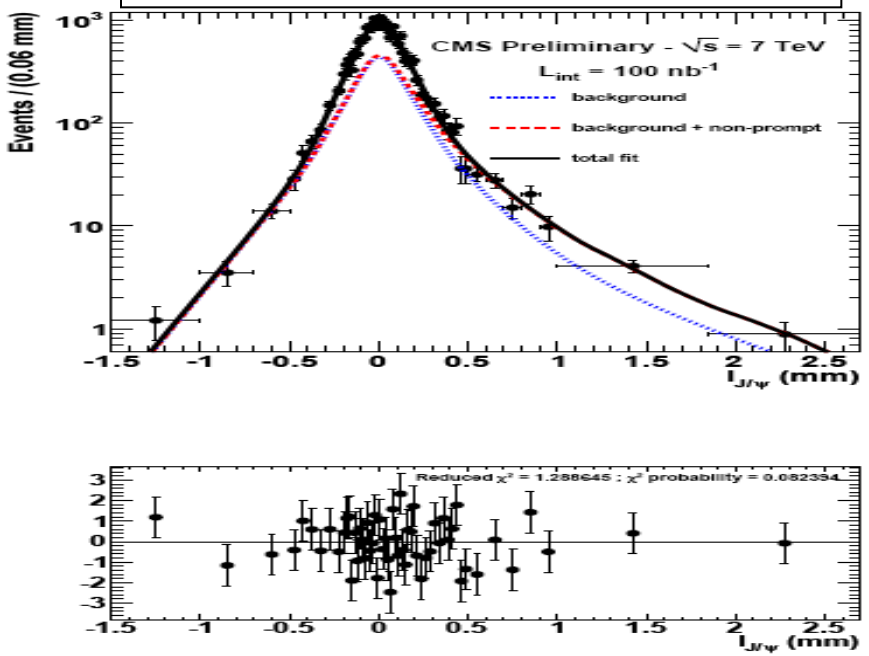

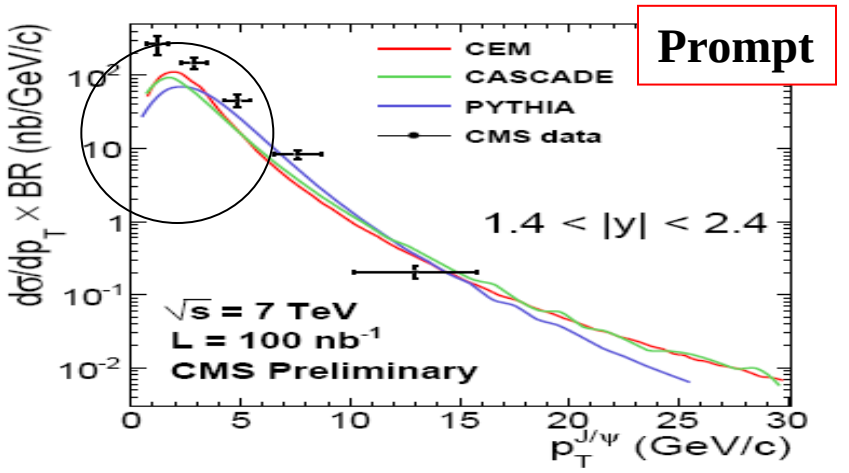

Prompt

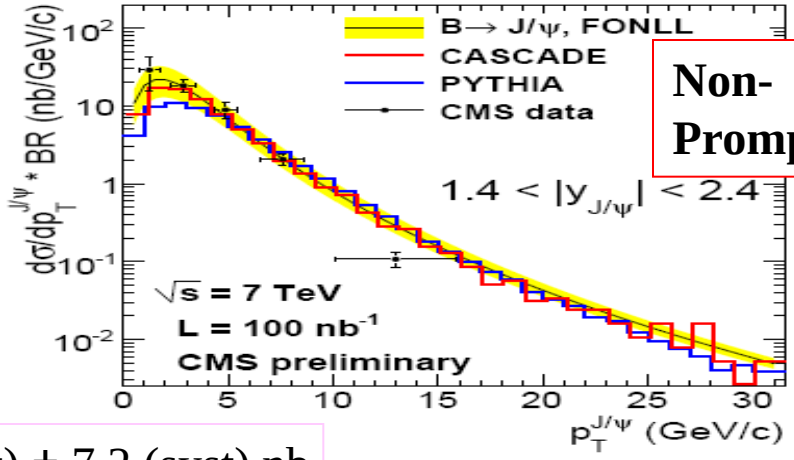

Non-Prompt

- Cross section for J/ψ production due to B-hadron decays 4< p_T(J/ψ)<30 GeV/c, |y|<2.4

σ (J/ψ from B)*BR(J/ψ -> μ+ μ-)=56.1 ± 5.5 (stat) ± 7.2 (syst) nb

Upsilon production cross section

- Theoretical predictions for Y more robust than for charmonium due to heavier b quark
- Selection similar to J/ψ
- Kinematic cuts

$$p_{\mathrm{T}}^{\mu} > 3.5 \text{ GeV}/c \quad \text{if} \quad |\eta^{\mu}| < 1.6$$
$$p_{\mathrm{T}}^{\mu} > 2.5 \text{ GeV}/c \quad \text{if} \quad 1.6 < |\eta^{\mu}| < 2.4$$

- Efficiencies computed using T&P technique on J/ψ sample, reweighing for different p_T distribution
- Acceptance and efficiencies in $p_T(\mu)$, η (μ) bins applied event by event.

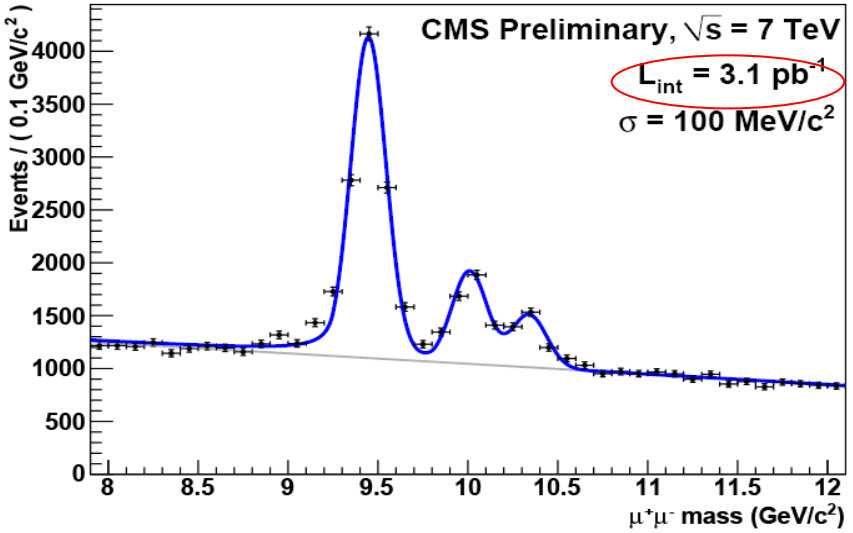

- Signal extraction EUML fit to mass distribution in $p_T(Y)$ bins to 3Crystal ball +linear function for background
- Common resolution for 3 peaks
- Y(1S) mass free parameter, ΔM of the others fixed by PDG

Upsilon production cross section

- Results for 280 nb-1 of data, assuming zero polarization

$$\sigma(pp \to \Upsilon(1S)X) \cdot \mathcal{B}(\Upsilon(1S) \to \mu^+\mu^-) = (8.3 \pm 0.5 \pm 0.9 \pm 1.0)\,|y| < 2.0$$

$$R = [\sigma(pp \to \Upsilon(2S)X) + \sigma(pp \to \Upsilon(3S)X)]/\sigma(pp \to \Upsilon(1S)X) = 0.44 \pm 0.06 \pm 0.07$$

- Main source of systematic uncertainty in Y(1S) production cross section is determination of muon identification efficiency (will be reduced with additional data) and luminosity.

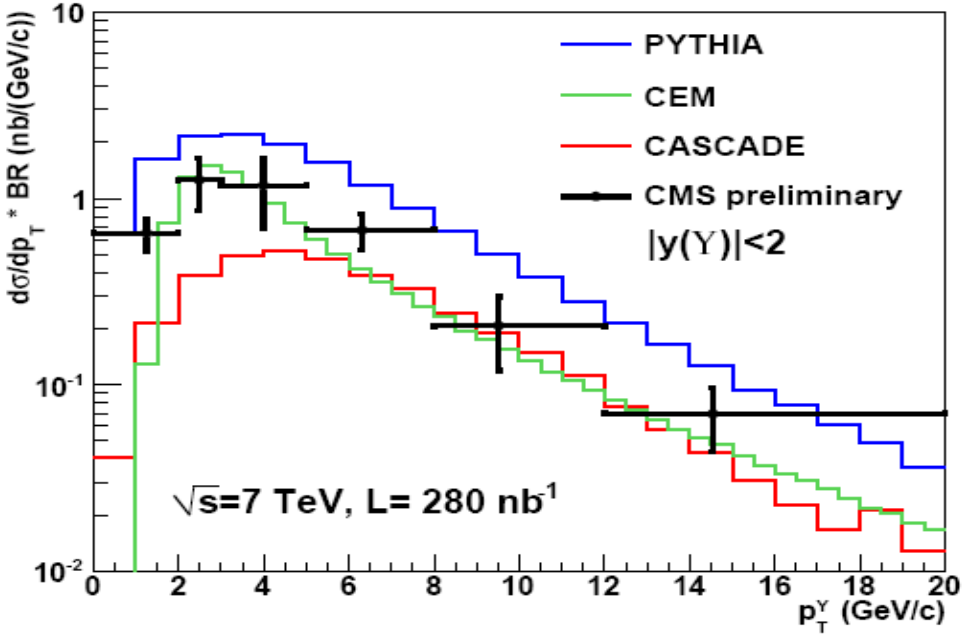

b-production

- Recent progress in theoretical understanding of b-quark production (in particular fragmentation) but theoretical uncertainties still sizeable
- Big interest in verifying the results at LHC energies, high cross section for bb production, accessing new regions in phase space.
- In addition events containing b-quarks are important background for many searches.
- Two methods for measuring inclusive b-production cross section, with different kinematic reaches and systematic uncertainties:
  - Muon tagging
  - Jet tagging

b-production at LHC

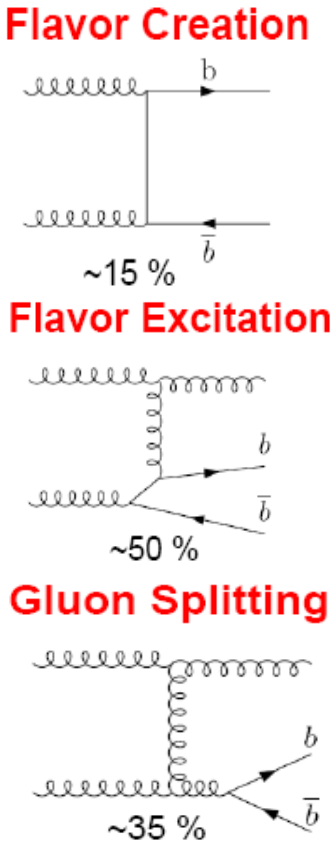

b-production with muons

- In semileptonic decay of b-quarks into muons and jets, the transverse momentum of the muon wrt closest track jet discriminates b events from background
  - Tracks clustered in jets with anti-kT with R=0.5

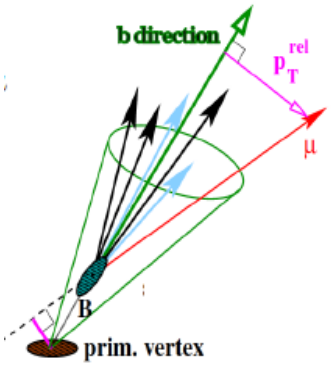

- Binned log-likelihood fit of the observed p_T^{rel} to obtain f_b from data
  - Signal and c-template from simulation
  - udsg background dominated by hadrons misidentified as muons, determined from data

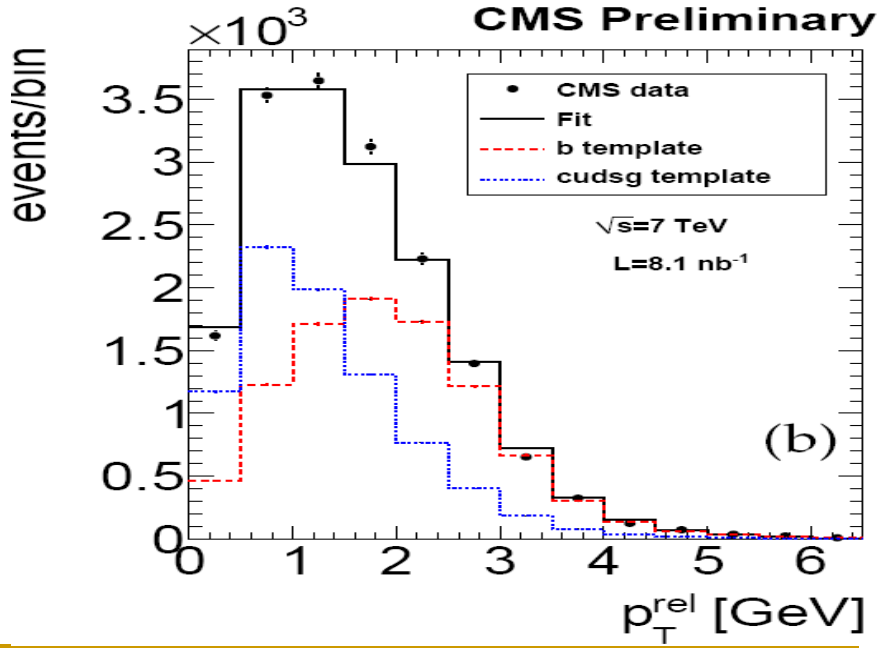

b-production with muons

- Trigger efficiency (single muon trigger) from data with minimum bias events.
- Muon reconstruction efficiency, b-jet finding efficiency, fake rate from simulation.
- Systematic uncertainties dominated by description of the udsg background and of the underlying event and by luminosity

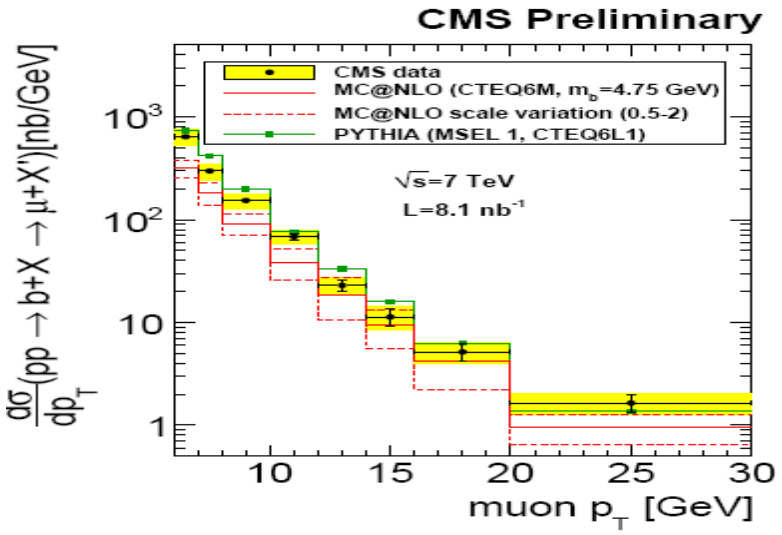

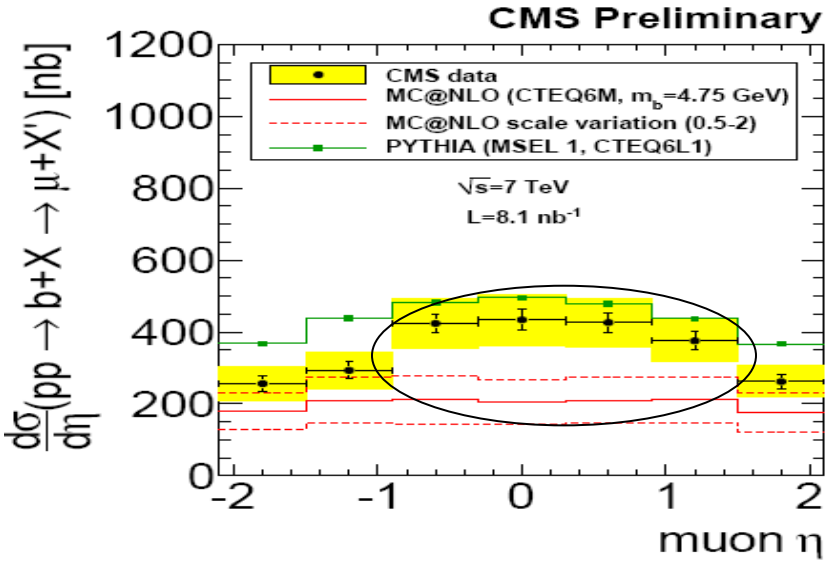

$$\sigma \equiv \sigma(pp \to b + X \to \mu + X', p_{\mu}^{\mu} > 6\,\mathrm{GeV}, |\eta^{\mu}| < 2.1)$$
$$= (1.48 \pm 0.04_{\mathrm{stat}} \pm 0.22_{\mathrm{syst}} \pm 0.16_{\mathrm{lumi}})\ \mu\mathrm{b}$$

Lumi=8.1 nb^{-1}

b-production with jet b-tagging

- Reconstruct PF jets in $18<p_T<300$ GeV with anti-kT in R=0.5, with $|y|<2.0$
- b-jets identified with secondary vertex tagger

- Secondary vertices (SV) from b- and c/light-quark decays can be distinguished by their relative distance from the primary vertex using a 3D decay length significance

Signed decay length of secondary vertexes

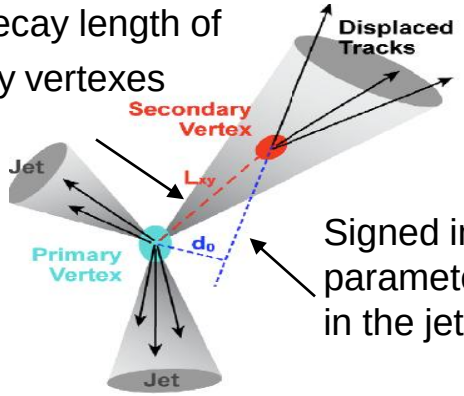

Signed impact parameter of tracks in the jet

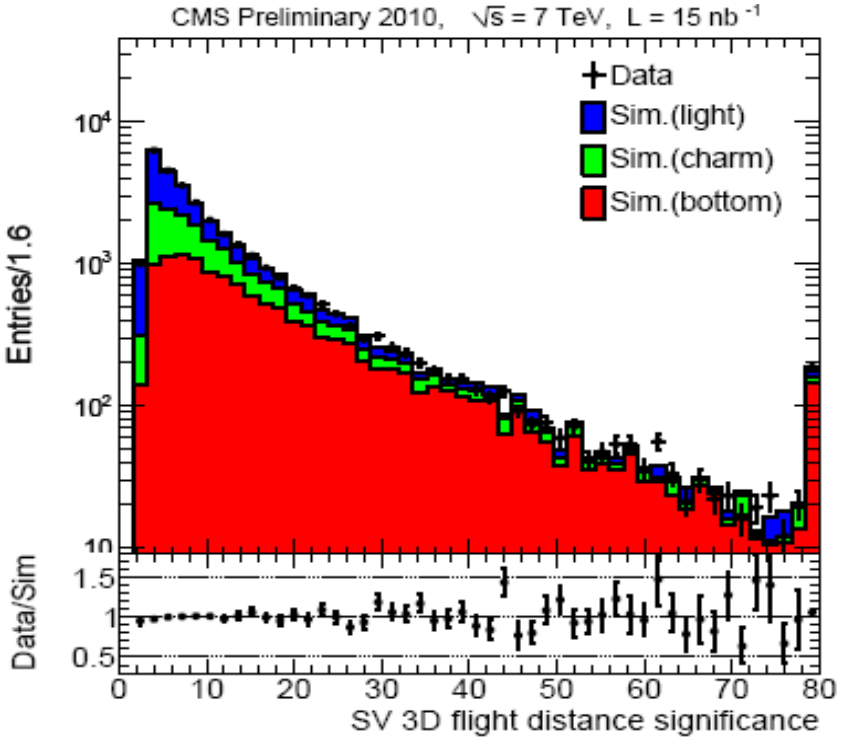

b-production with jet b-tagging

$$\frac{d^2\sigma_{\mathrm{b-jets}}}{dp_T dy} = \frac{N_{\mathrm{tagged}} f_b C_{\mathrm{smear}}}{\epsilon_{\mathrm{jet}} \epsilon_b \Delta p_T \Delta y \mathcal{L}}$$

18<pT<300 GeV, |y|<2.0

- N_{tagged}= Measured number of tagged jets per (p_T,η) bin.
- f_b = fraction of tagged jets containing a b-hadron (purity)
- ε_b= efficiency of tagging b-jets
- ε_{jet}= jet reconstruction efficiency
- C_{smear}=unfolding correction from measured p_T back to particle level
- f_b, ε_b, ε_{jet} calculated from MC in (p_T,η) bins, in agreement with data estimations.

b-tagging efficiency

- Efficiency of tagging b-jets from simulation.
- Measured in the data using semileptonic decays of b-> μ+jets. Fit p_T^{rel} both in b-tagged and in non b-tagged sample. Efficiency given by ratio of corresponding Nb

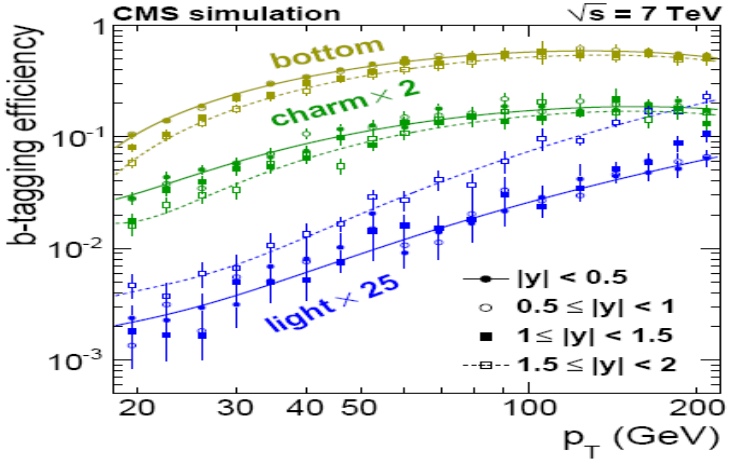

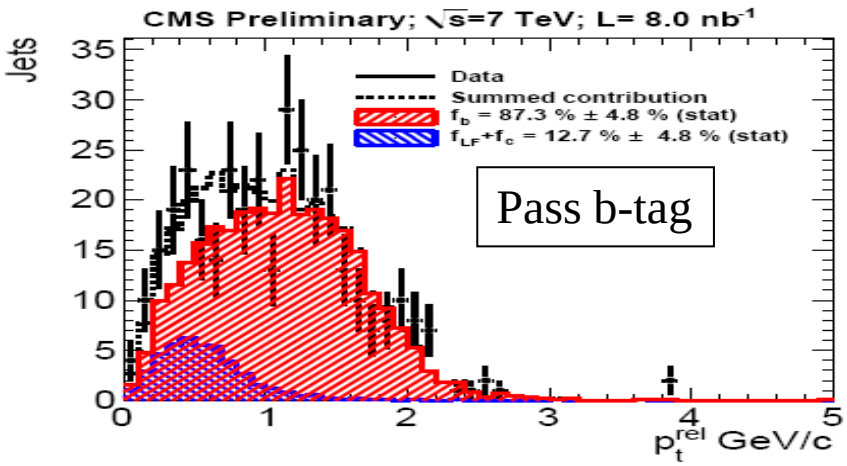

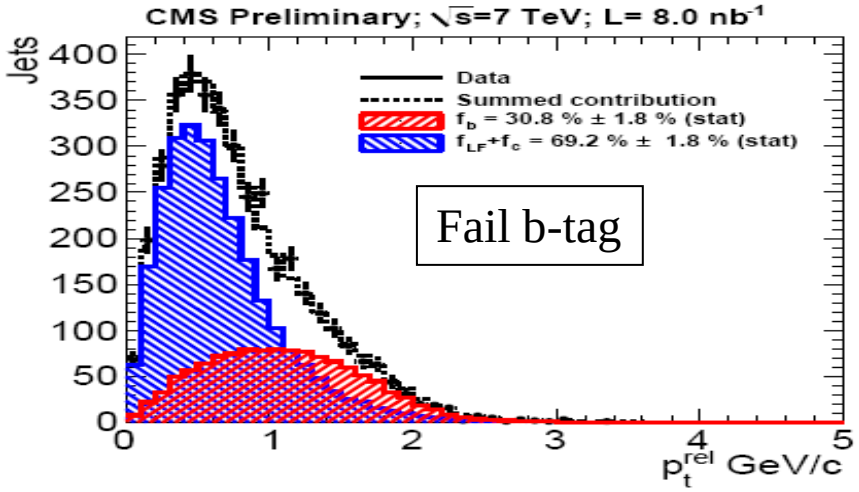

- Data/MC ratio: 1 within 20% statistical uncertainty.

b-tagging purity

- Data estimate: Compute invariant mass of tracks associated to SV computed after selection. Fit performed, taking shapes for light, c, b from simulation.
- Good data/MC agreement

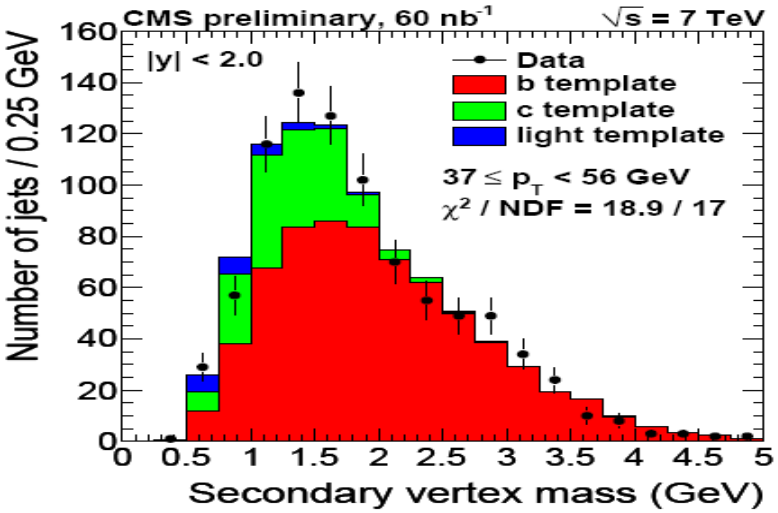

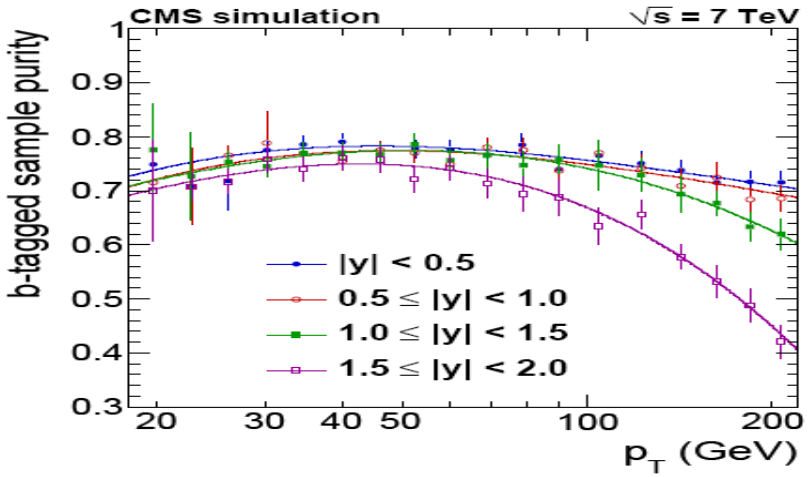

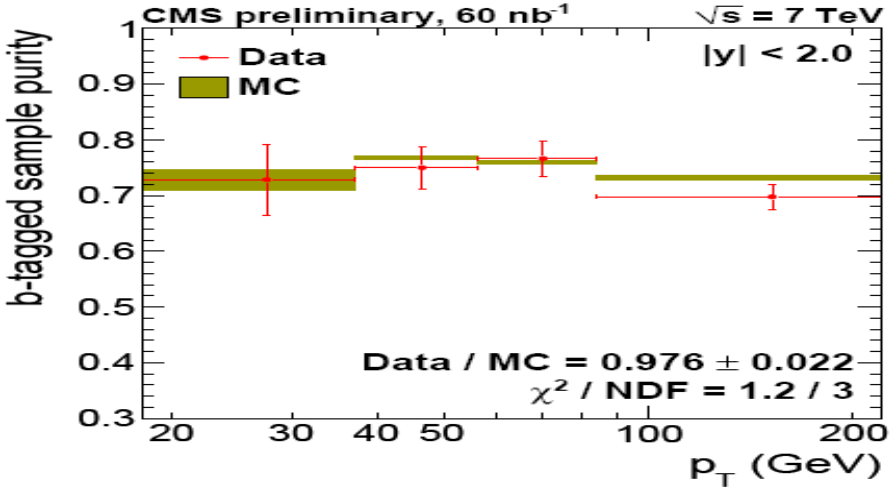

Inclusive b production with b-tagging

- Leading uncertainties: jet energy scale, luminosity, b-tag efficiency and mistag rates.

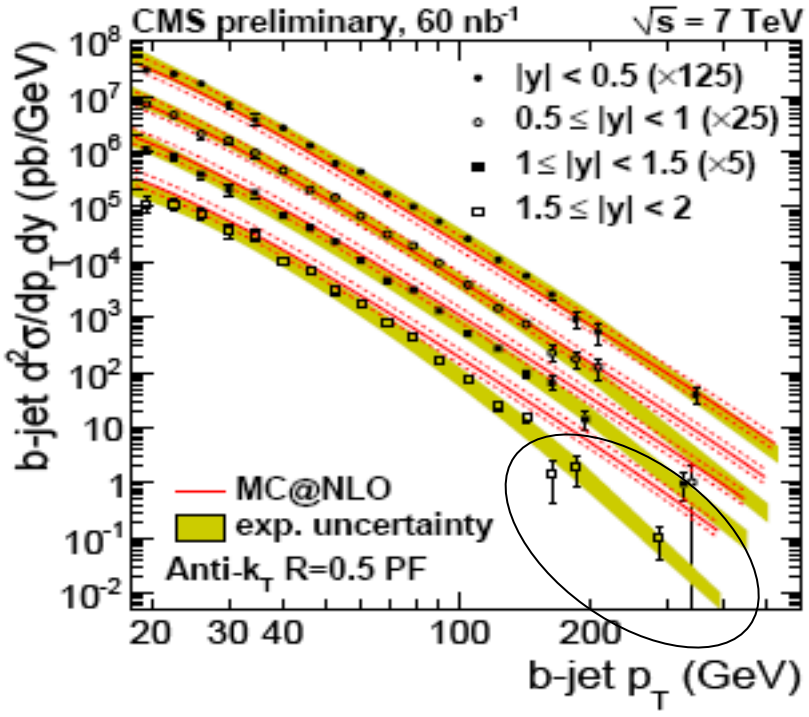

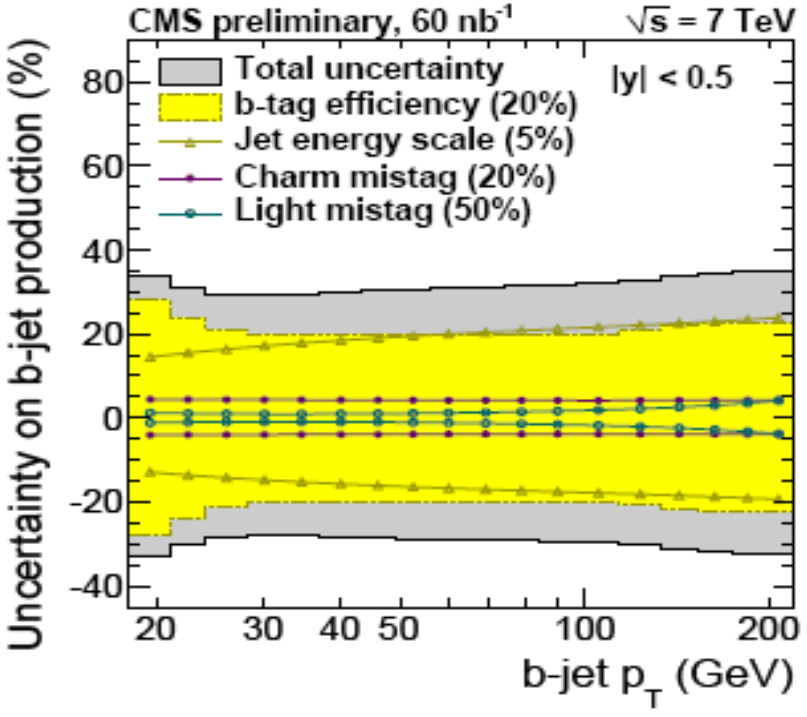

Ratio b-jet to inclusive jet production

- Luminosity and jet energy scale uncertainties cancel out in the ratio
- Leading uncertainties from b-tag efficiency and charm mistag rates. These are statistical uncertainties from data-driven methods.

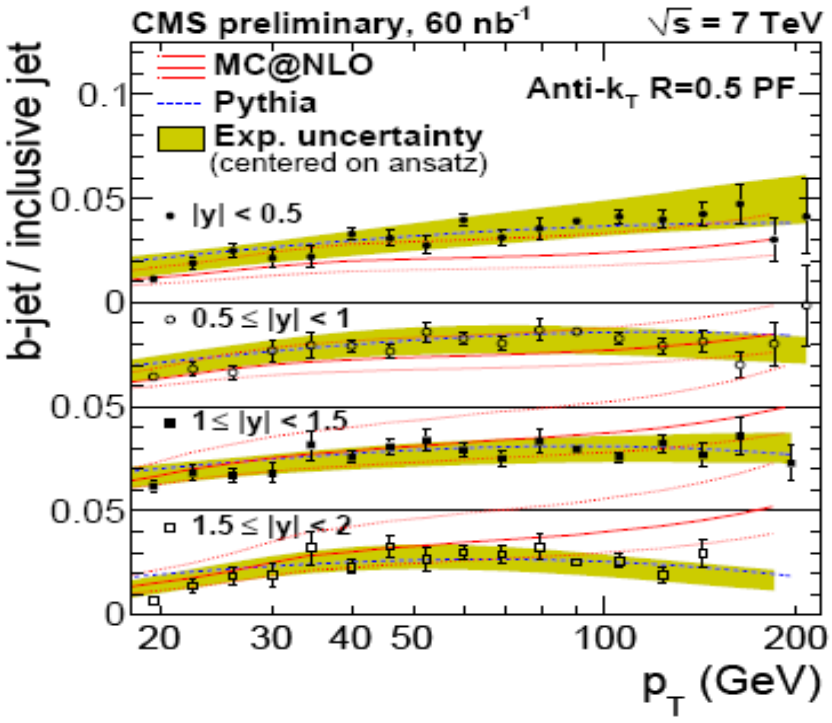

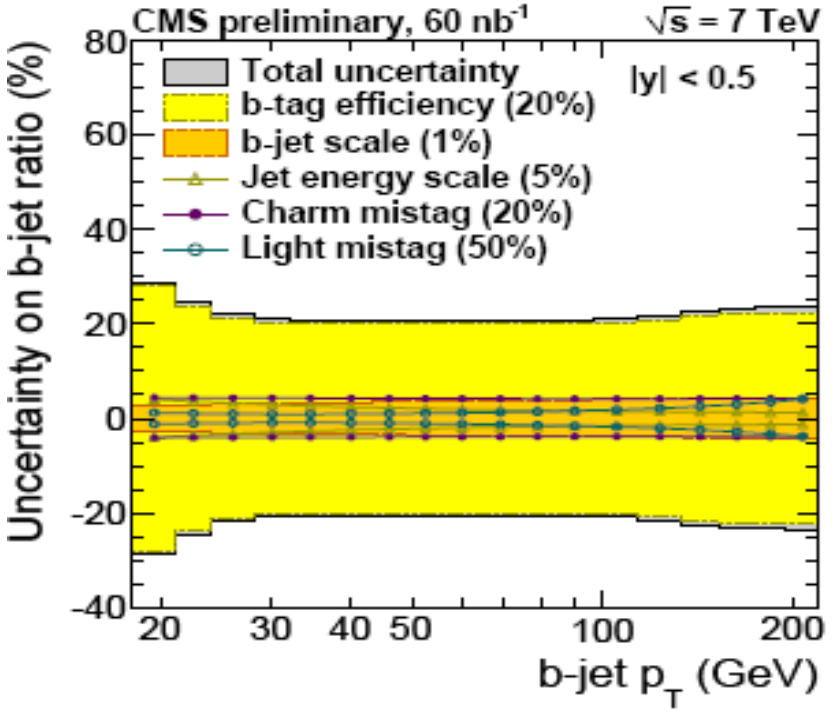

Conclusions

- Very good tracking and muon detector performance allow rich quarkonia and B-Physics program at CMS.
  - First measurements of J/ψ and Υ cross sections at 7 TeV available.
- Very good b-tagging performance from early stage already! Measurement of inclusive b-production cross section has been possible with this method
- And much more to come!

Main references

- CMS PAS BPH-10-002. J//ψ prompt and non-prompt cross sections in pp collisions at $\sqrt{s}$ = 7TeV
- CMS PAS BPH-10-003. Upsilon production cross section in pp collisions at $\sqrt{s}$ = 7TeV
- CMS PAS BPH-10-007. Open beauty production cross section with muons in pp collisions at $\sqrt{s}$ = 7TeV
- CMS PAS BPH-10-009. Inclusive b-jet production in pp collisions at $\sqrt{s}$ = 7TeV
- CMS PAS BTV-10-001. Commissioning of b-jet identification with pp collisions at $\sqrt{s}$ = 7TeV
- CMS PAS MUO-10-002. Performance of muon identification in pp collisions at $\sqrt{s}$ = 7TeV
- CMS PAS TRK-10-002 Measurement of tracking efficiency.
- CMS PAS JME-10-001. Jets in 0.9 and 2.36 TeV collisions

Back Up

First exclusive B channels

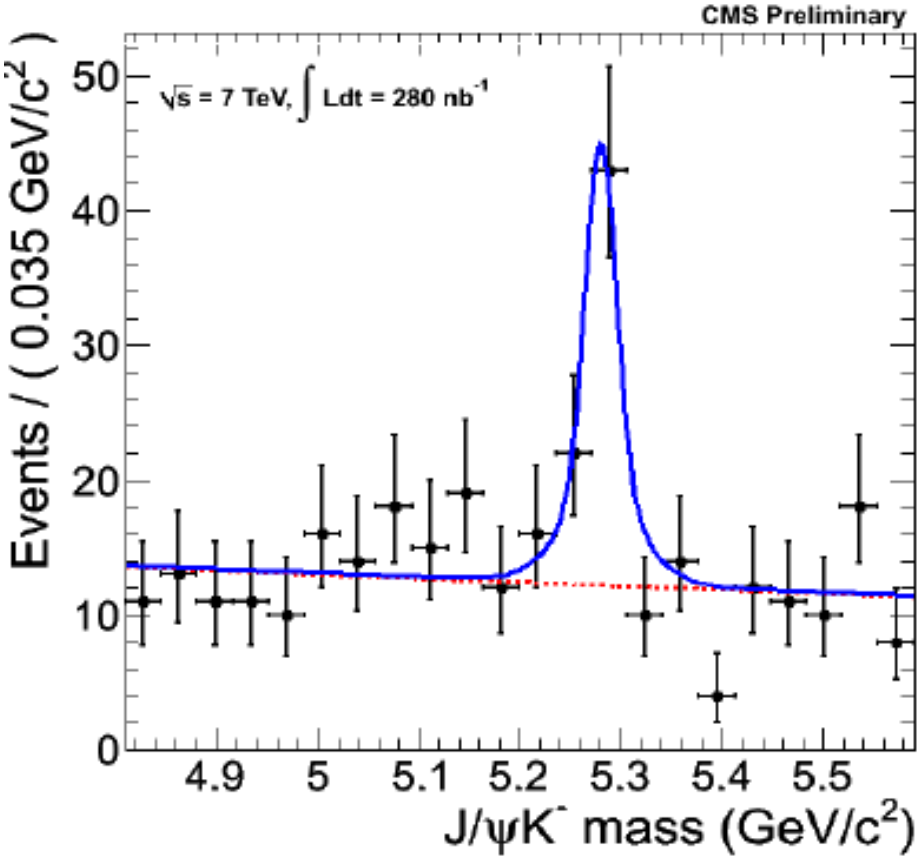

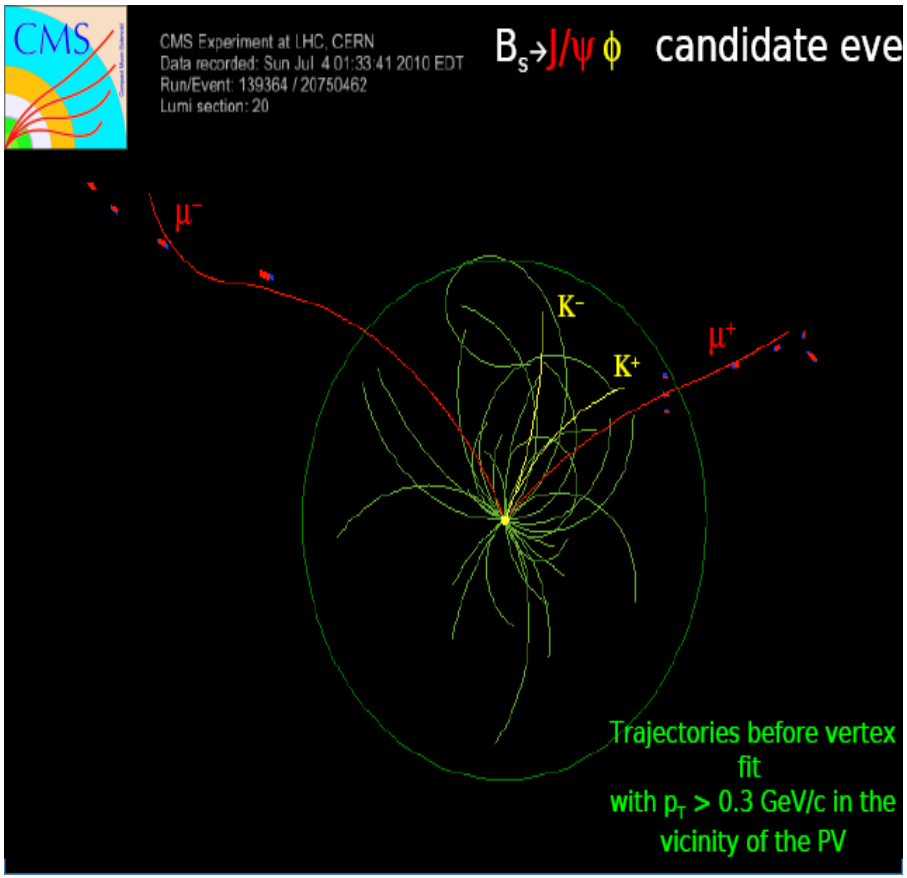

b-tagging input variables Data/MC

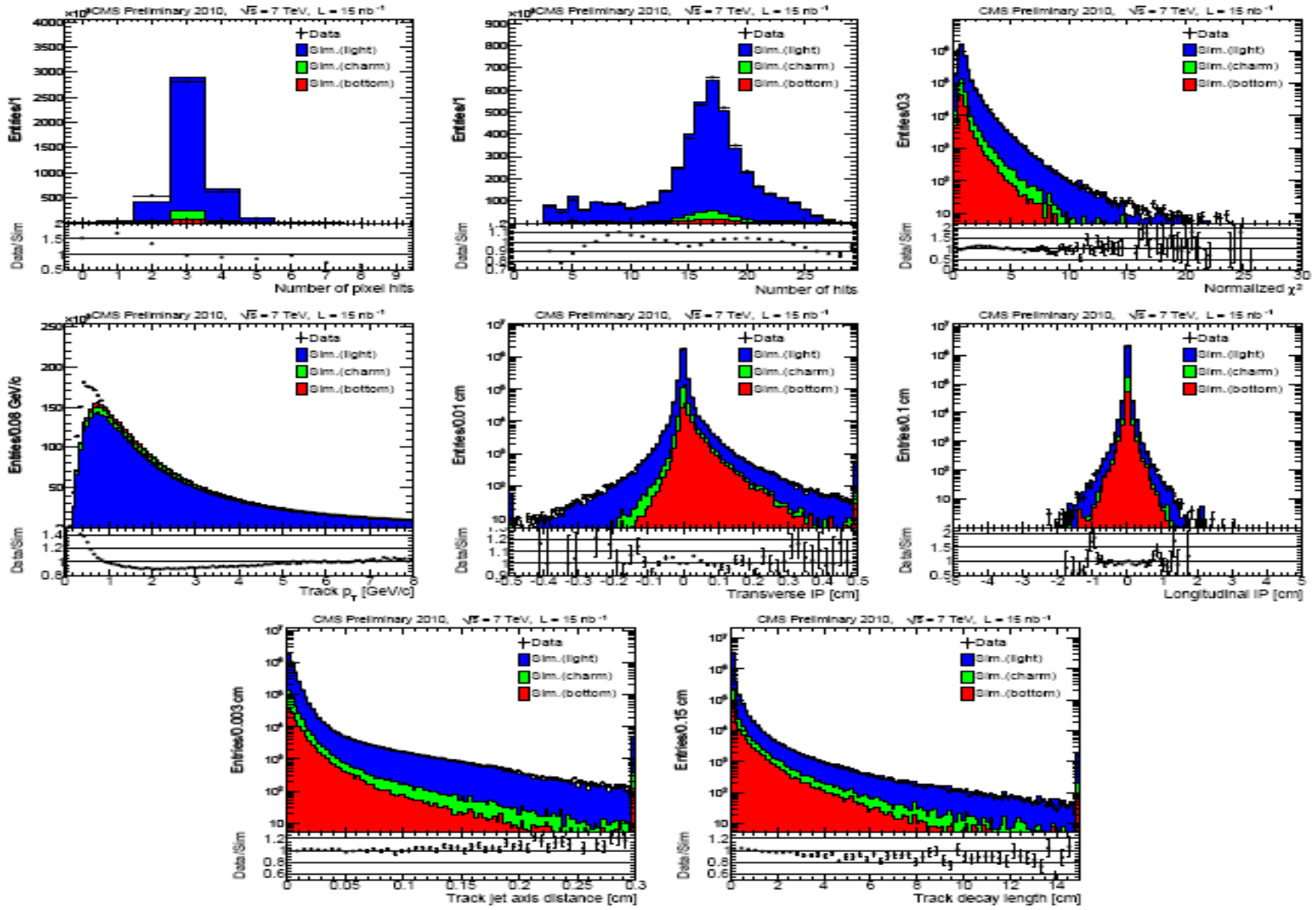

b-tagging

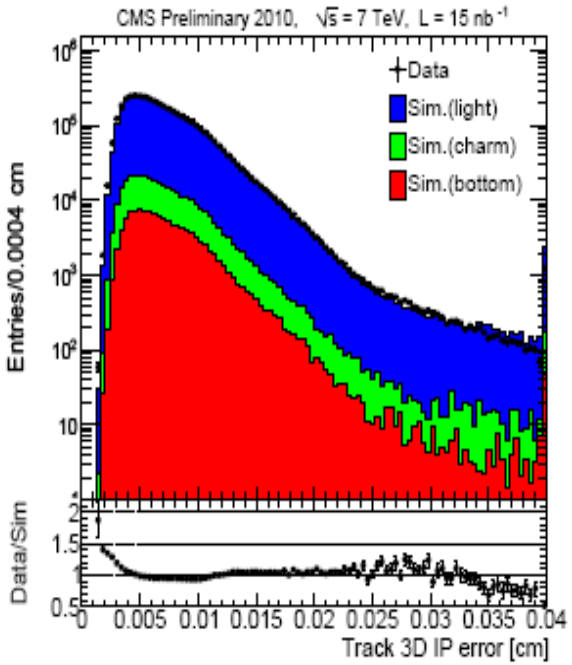
CMS Preliminary 2010, √s = 7 TeV, L = 15 nb⁻¹
Data
Sim.(light)
Sim.(charm)
Sim.(bottom)
Entries/0.0004 cm
Data/Sim
Track 3D IP error [cm]

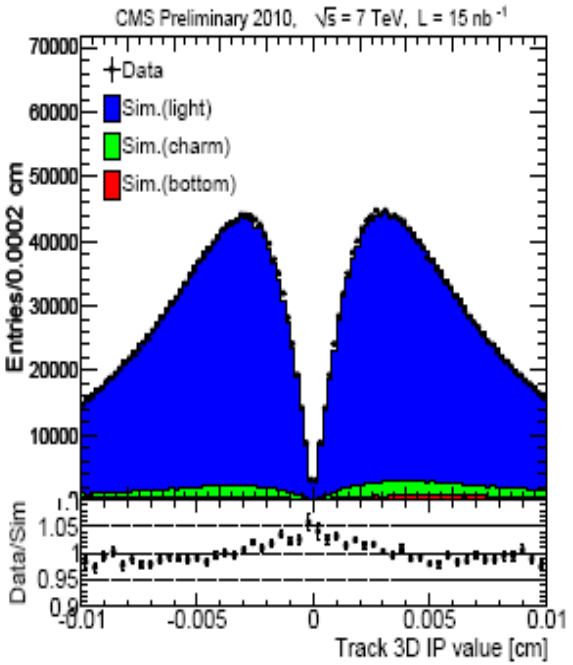
CMS Preliminary 2010, √s = 7 TeV, L = 15 nb⁻¹
Data
Sim.(light)
Sim.(charm)
Sim.(bottom)
Entries/0.0002 cm
Data/Sim
Track 3D IP value [cm]

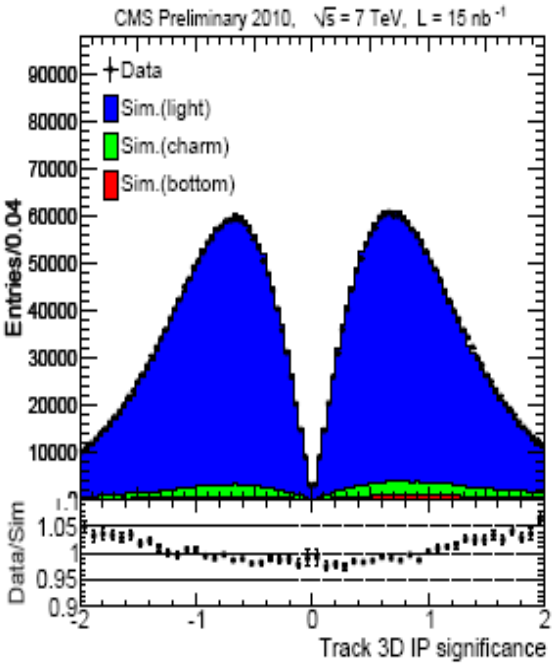
CMS Preliminary 2010, √s = 7 TeV, L = 15 nb⁻¹
Data
Sim.(light)
Sim.(charm)
Sim.(bottom)
Entries/0.04
Data/Sim
Track 3D IP significance

b-tagging

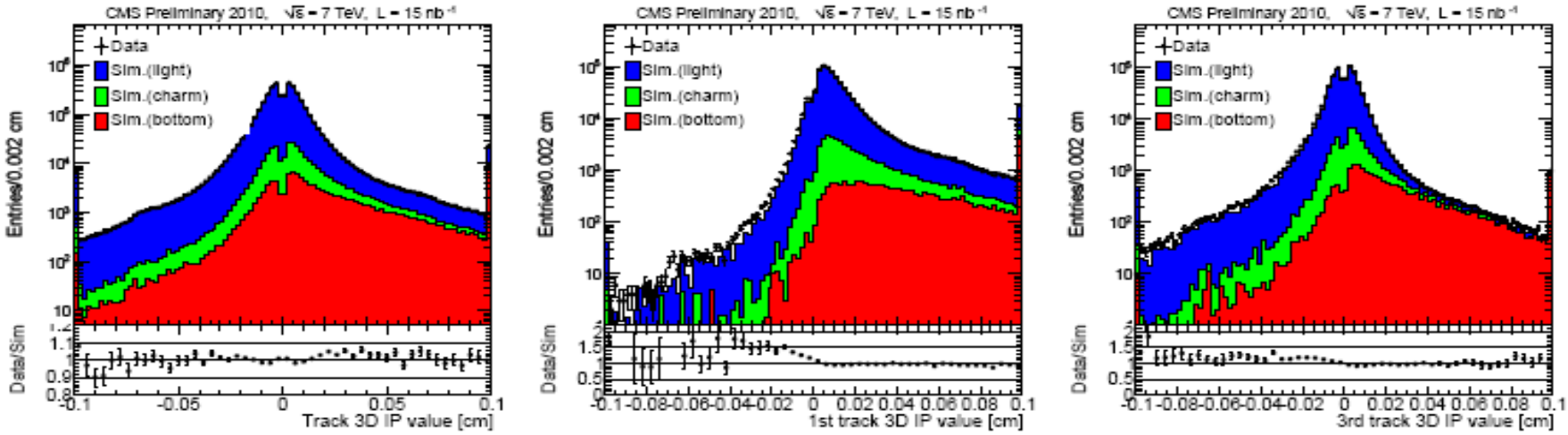

Figure 5: from left to right: IP value for all selected tracks, 1st, and 3rd track, in the selected jets.

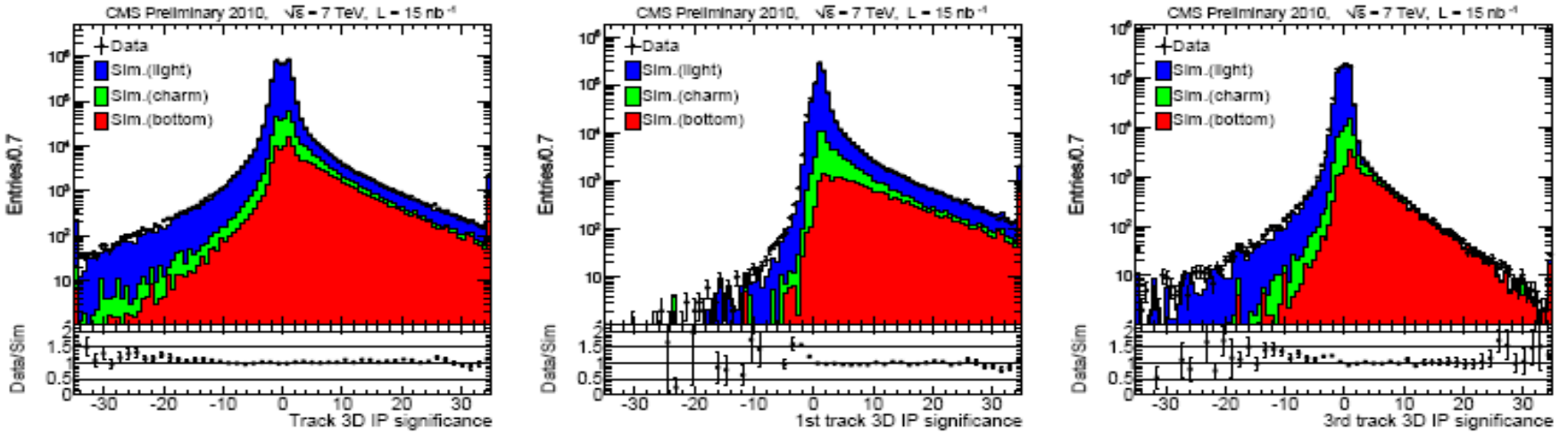

Figure 6: from left to right: IP significance for all selected tracks, 1st, and 3rd track, in the selected jets.

b-tagging

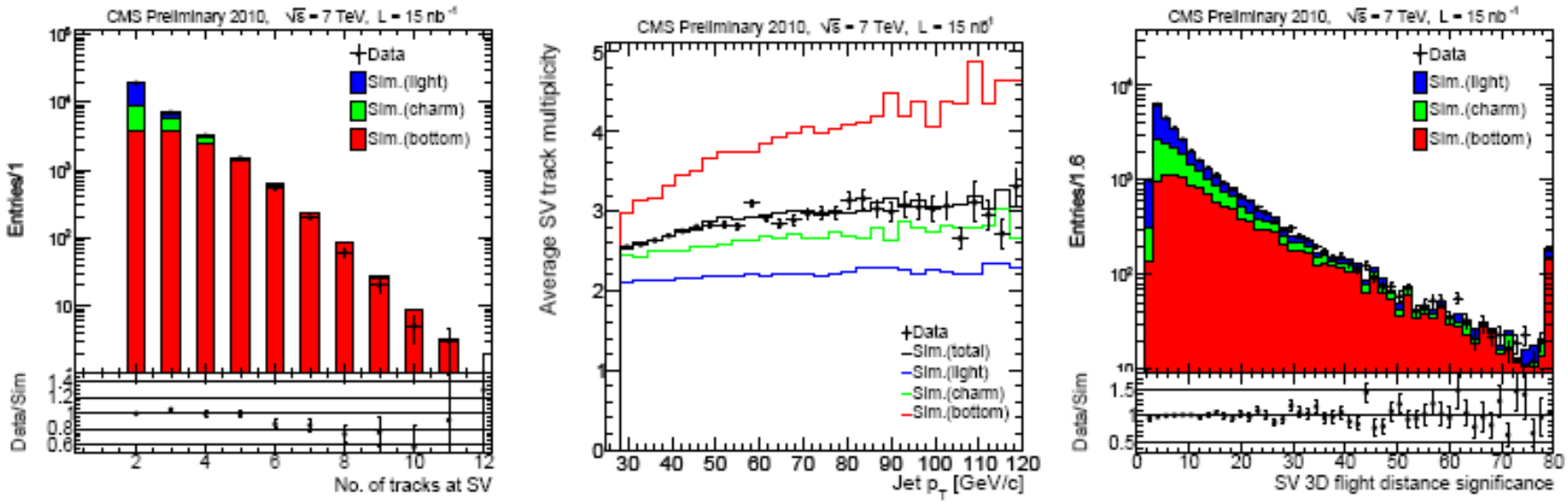

Figure 7: Secondary vertex properties: (left) number of tracks; (middle) average number of tracks vs p_T; (right) flight distance significance.

b-tagging

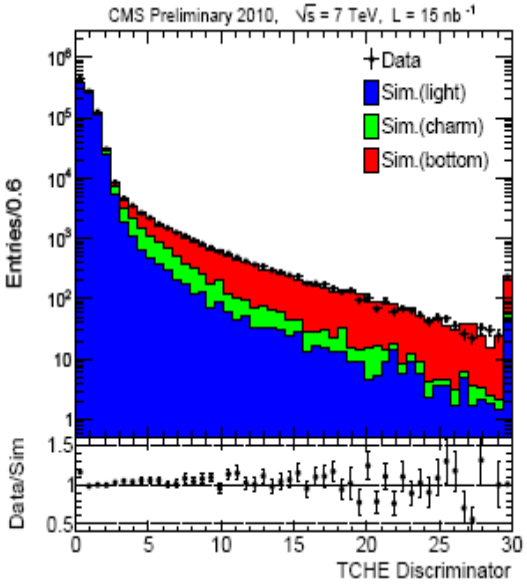
CMS Preliminary 2010, √s = 7 TeV, L = 15 nb⁻¹
Data
Sim.(light)
Sim.(charm)
Sim.(bottom)
Entries/0.6
Data/Sim
TCHE Discriminator

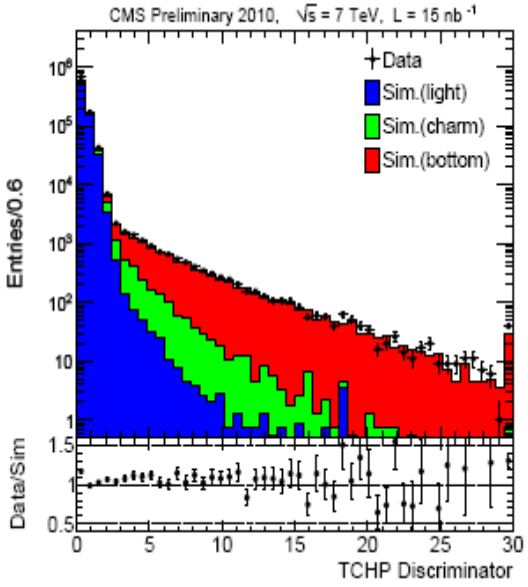
CMS Preliminary 2010, √s = 7 TeV, L = 15 nb⁻¹
Data
Sim.(light)
Sim.(charm)
Sim.(bottom)
Entries/0.6
Data/Sim
TCHP Discriminator

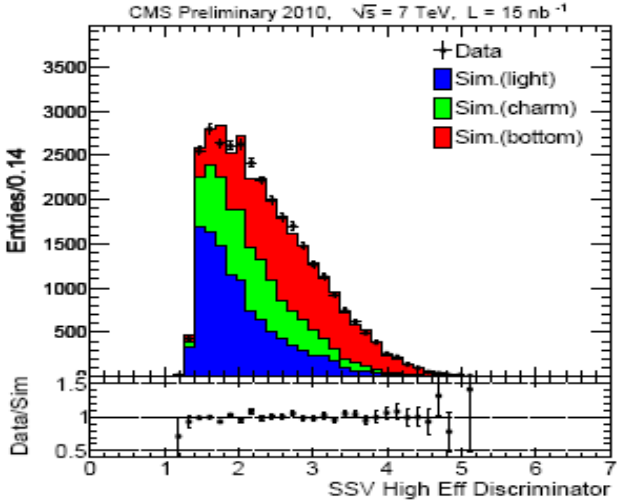
CMS Preliminary 2010, √s = 7 TeV, L = 15 nb⁻¹
Data
Sim.(light)
Sim.(charm)
Sim.(bottom)
Entries/0.14
Data/Sim
SSV High Eff Discriminator

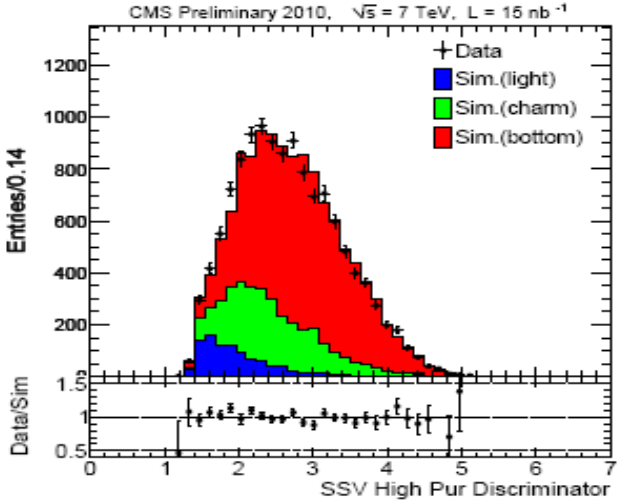
CMS Preliminary 2010, √s = 7 TeV, L = 15 nb⁻¹
Data
Sim.(light)
Sim.(charm)
Sim.(bottom)
Entries/0.14
Data/Sim
SSV High Pur Discriminator

Negative tags

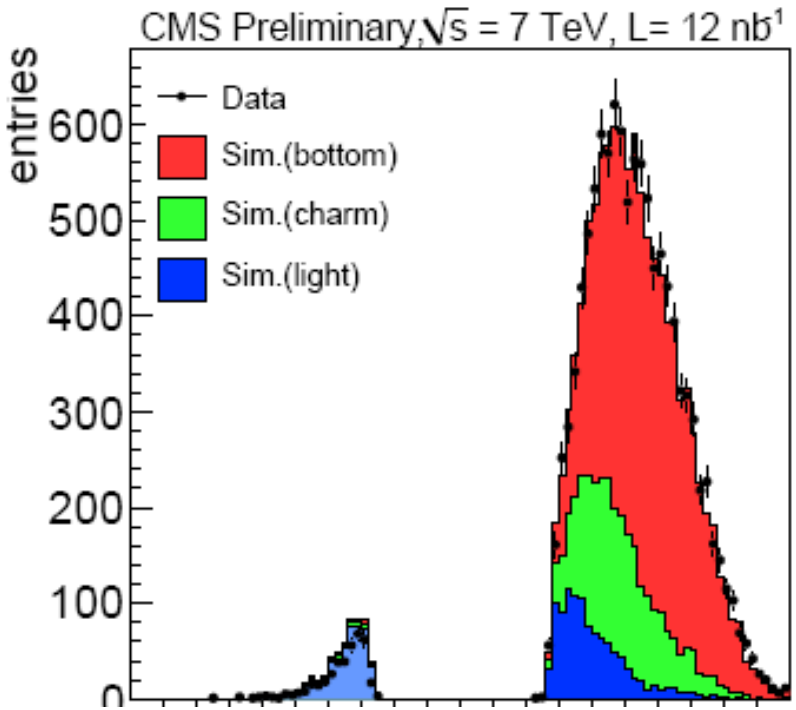

Figure 17: Negative and positive b tag discriminators in data (dots) and MC for LF jets with K^0_S and Λ reweighting (blue area), c jets (green area) and b jets (red area). The simulated distributions for negative and positive taggers are indicated by light and dark shading, respectively. Overflows are displayed in the upper bin.

Templates for b-tagging efficiency

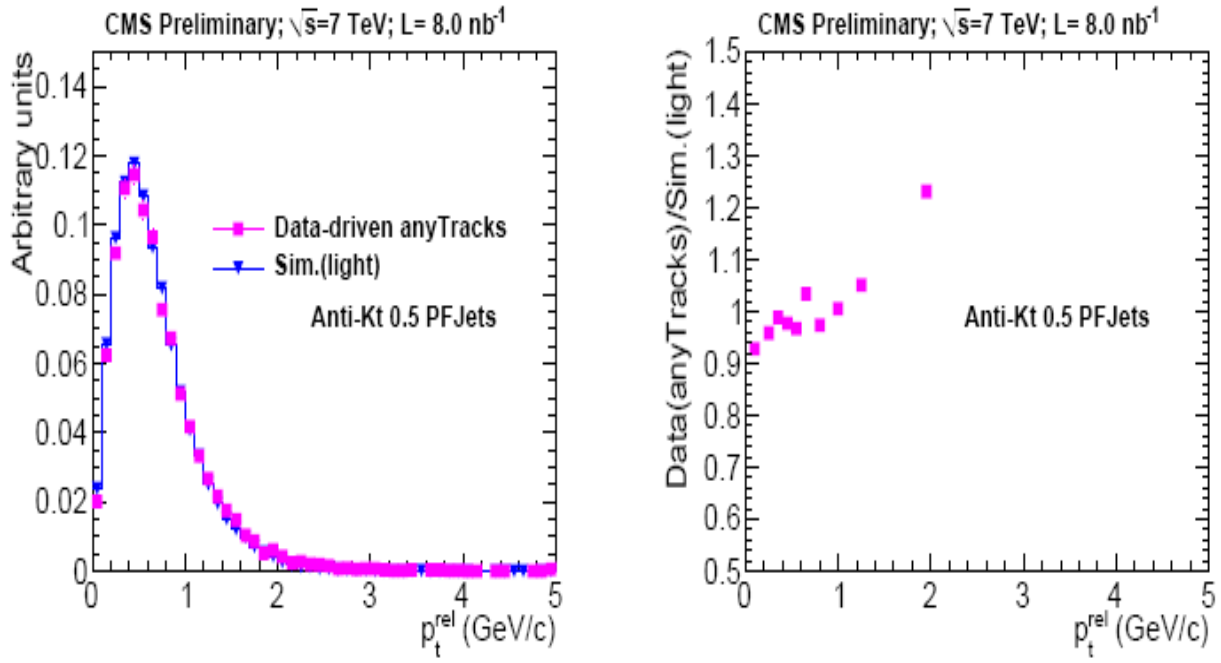

Figure 15: (Left) Comparison of muon p_T^{rel} templates for LF jets, obtained from data and from simulation with light jet flavour identification; (right) ratio of the templates shown on the left.

b-tagging, production mechanism

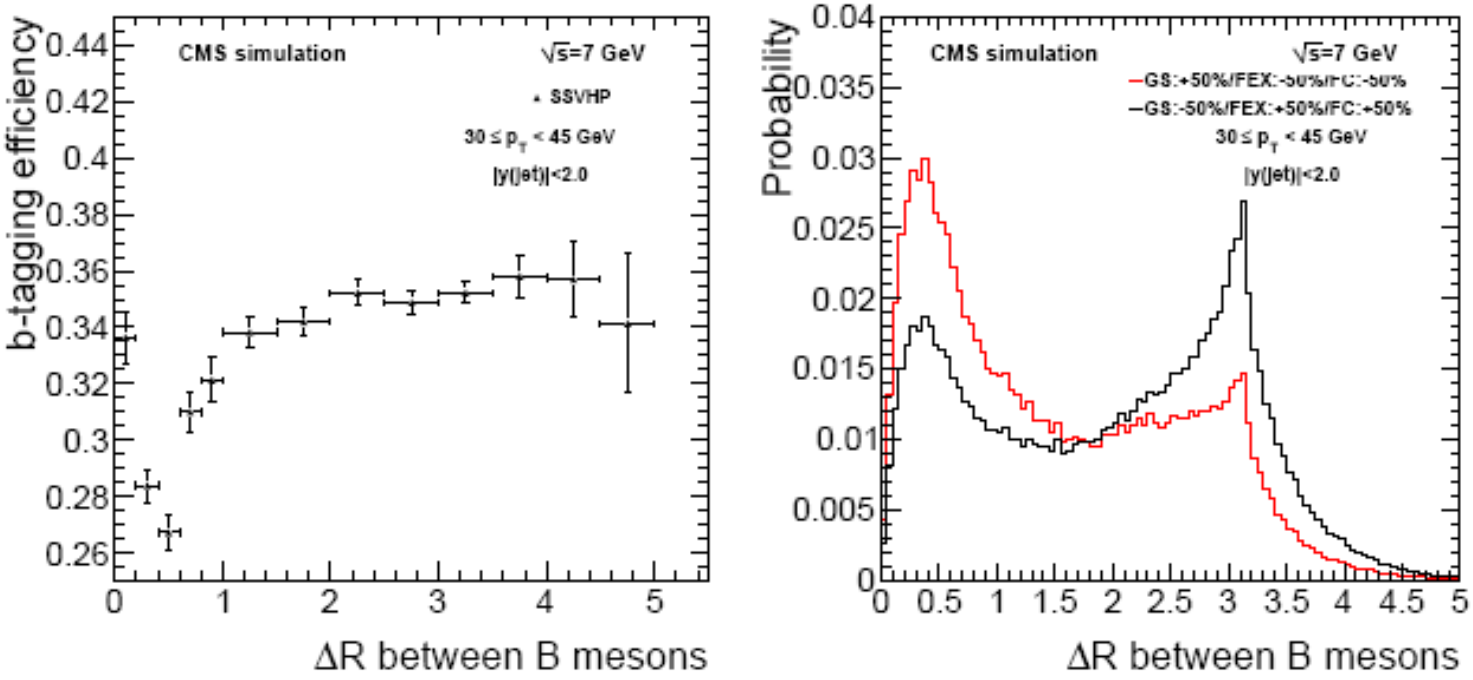

Figure 5: The b-tagging efficiency variation versus ΔR between b-hadrons (left). Distribution of ΔR between b-hadrons for $\pm 50\%$ variations of GS and FC+FEX (right).

J/Psi

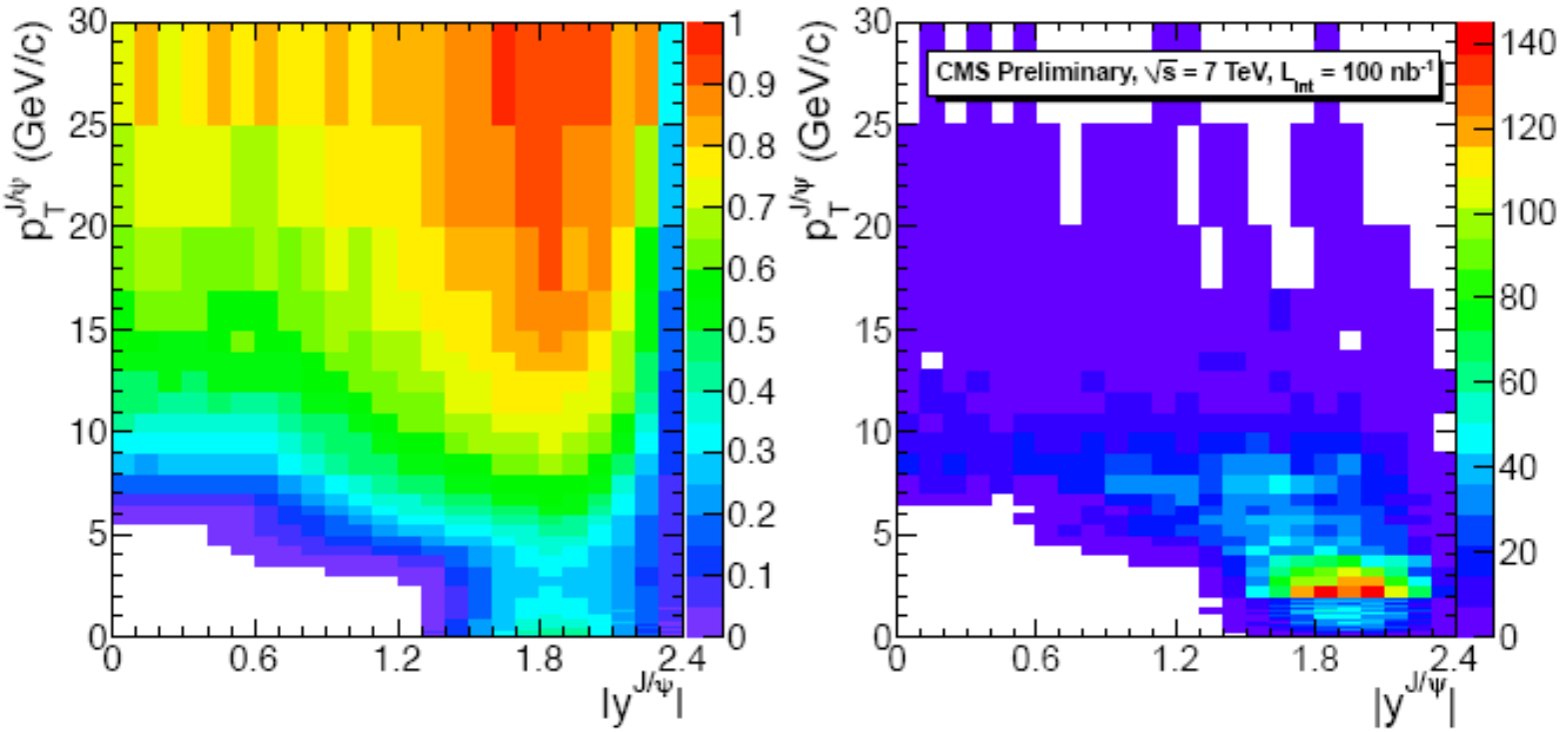

Figure 2: Left: Acceptance as a function of p_T and rapidity of the J/ψ. Right: Measured p_T versus $|y|$ two-dimensional distribution of the muon pairs within $\pm$ 100 MeV/c^2 from the nominal J/ψ mass.

Ks mass

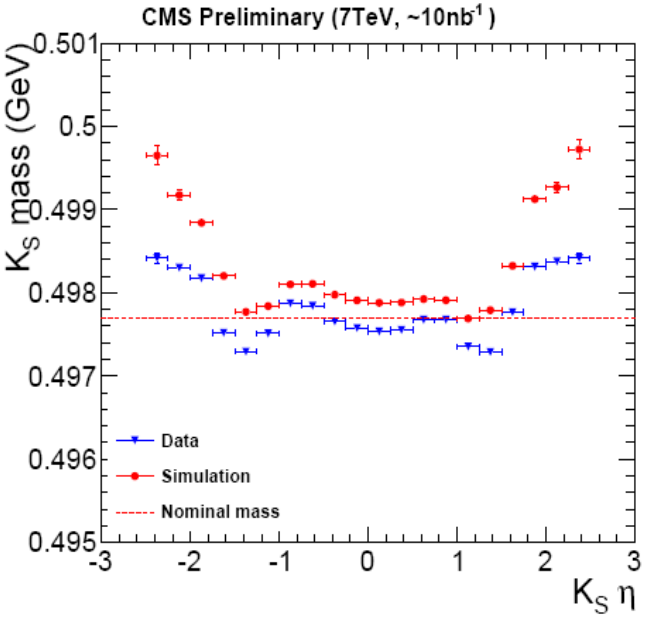
CMS Preliminary (7TeV, ~10nb^{-1})
K_S mass (GeV)
K_S η
Data
Simulation
Nominal mass

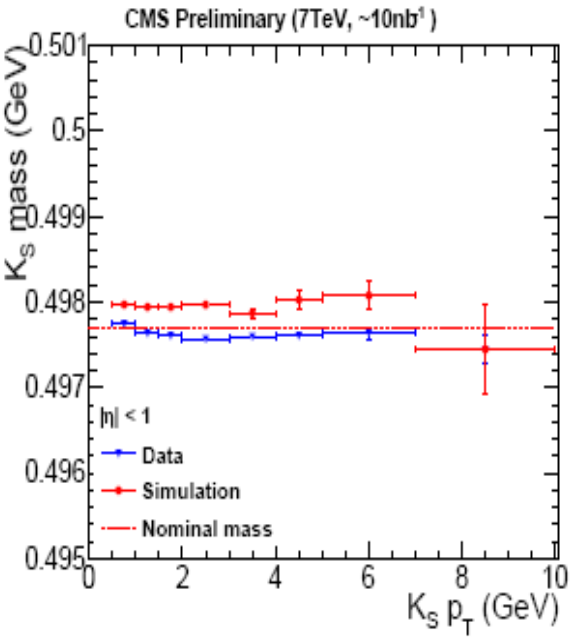
CMS Preliminary (7TeV, ~10nb^{-1})
K_S mass (GeV)
K_S p_T (GeV)
|η| < 1
Data
Simulation
Nominal mass

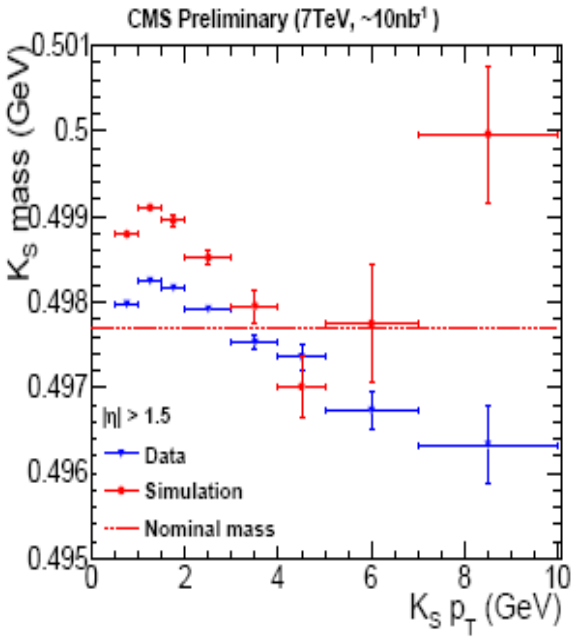
CMS Preliminary (7TeV, ~10nb^{-1})
K_S mass (GeV)
K_S p_T (GeV)
|η| > 1.5
Data
Simulation
Nominal mass

J/Psi mass

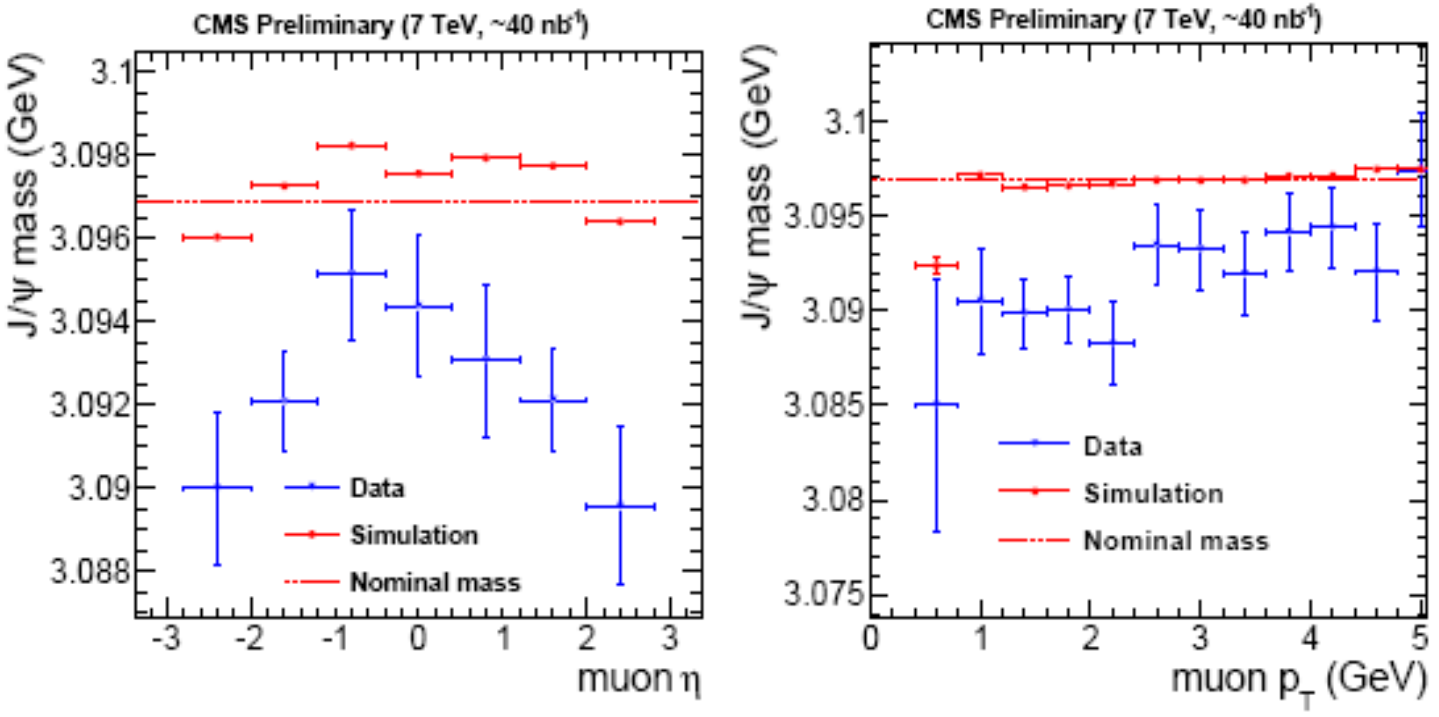

Figure 13: The J/ψ invariant mass as function of the η and p_T of the muons.

J/Psi mass

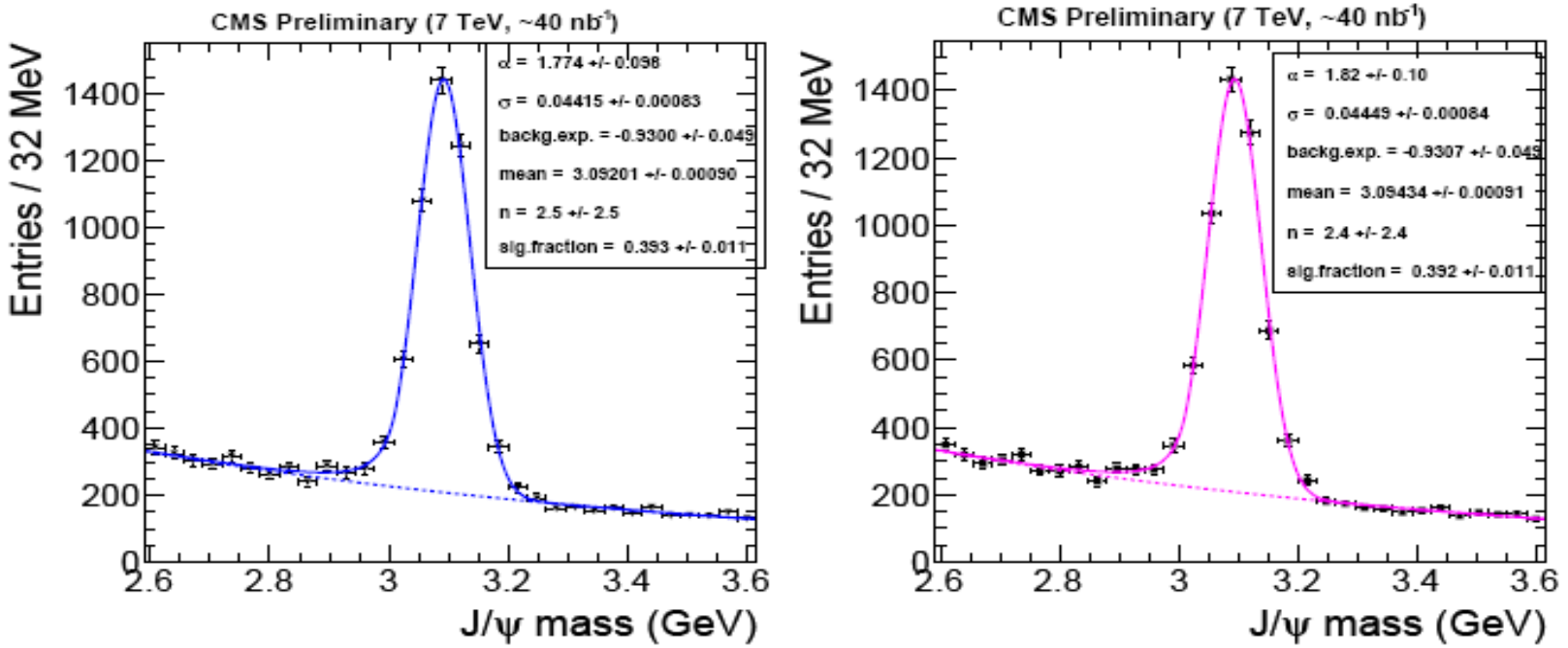

Figure 15: (Left) J/ψ mass distribution as measured with ~ 40 nb^{-1} of integrated luminosity. (Right) Same distribution after the correction of the momentum scale using the functions and parameters listed in Table 2. The fits are done with sum of an exponential for the background with a Crystal Ball function for the signal, taking into account also the tail due to the Final State Radiation

J/Psi mass

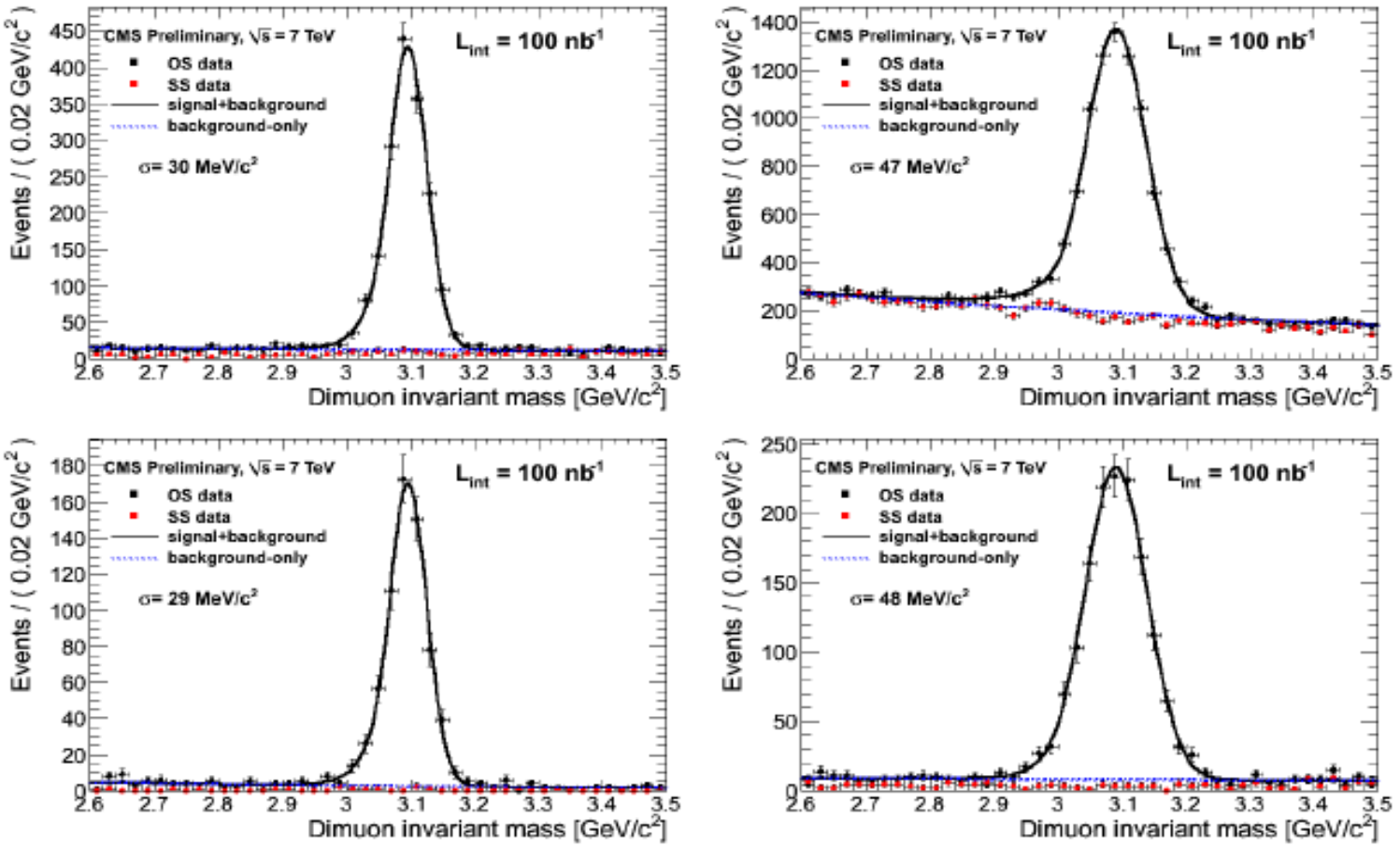

Figure 1: Dimuon invariant mass distributions for all categories (top) and for only Global Muon pairs (bottom), in the rapidity windows $|y| < 1.4$ (left) and $1.4 < |y| < 2.4$ (right). Also shown are the invariant mass widths from a fit of a Crystal Ball function plus an exponential. The worse mass resolution for large rapidities is caused by the smaller lever arm of the tracks. The non-peaking red distributions show the same sign dimuon combinations.

J/Psi: muon momentum resolution

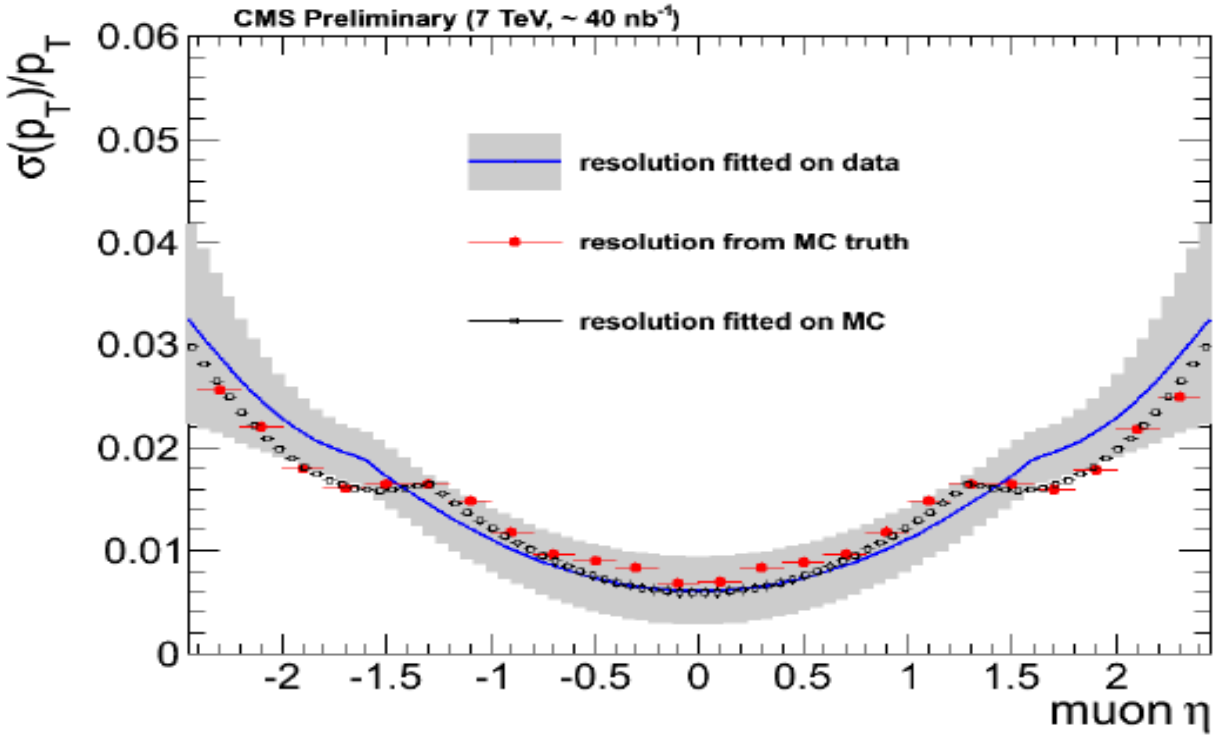

Figure 17: Resolution on transverse momentum as measured with $\sim$ 40 nb^{-1} of integrated luminosity (black line) compared to the Monte Carlo resolution computed from Monte Carlo truth (red points) and from the fit as described in Section 4.2 (black squares). The gray band in data represents the error on the fitted function for data computed from the errors on the parameters.

Upsilon

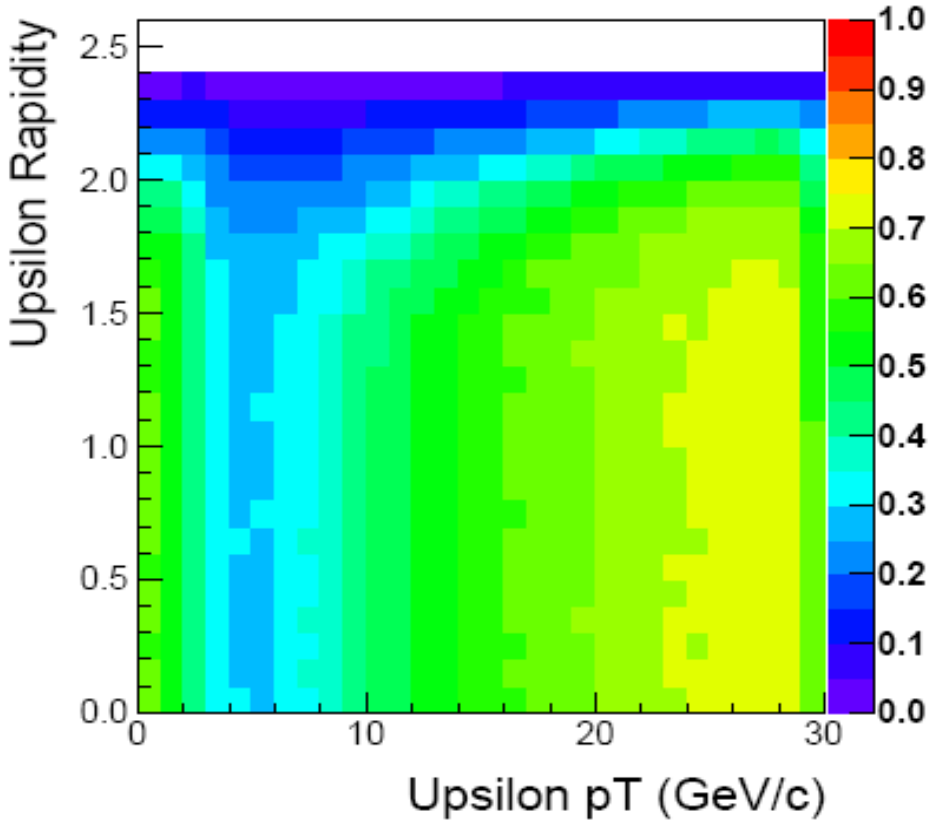

Figure 2: Unpolarized $\Upsilon(1S)$ acceptance as a function of p_T and y.

Muon ID efficiency

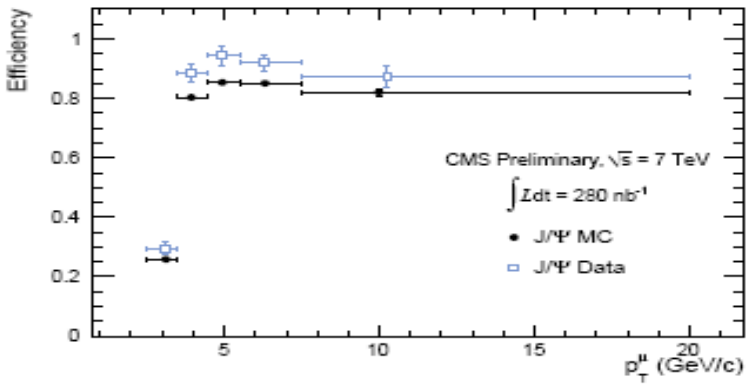

(a) Central region, $|\eta^\mu| < 1.2$

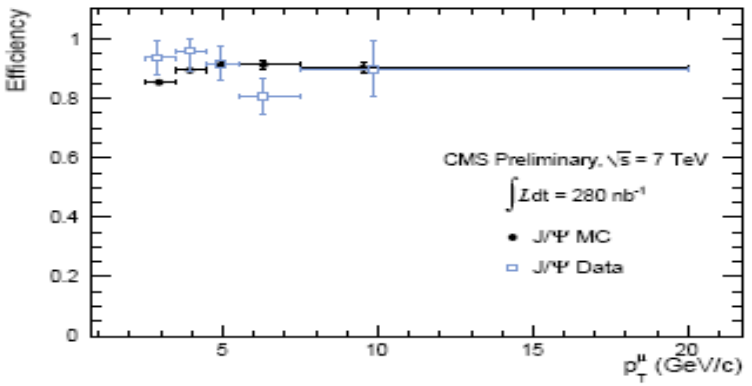

(b) Transition region, $1.2 < \eta^\mu < 1.6$

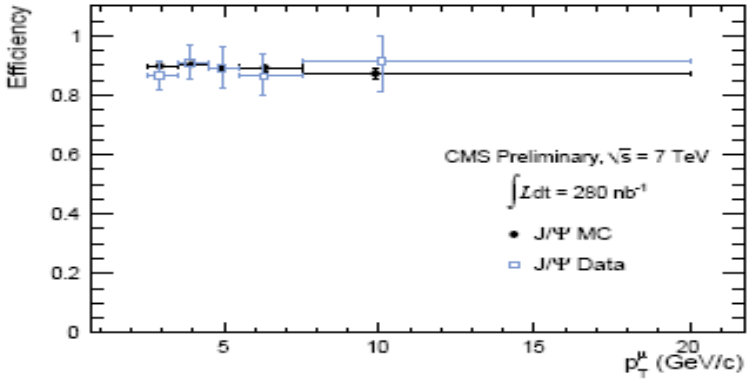

(c) Forward region, $1.6 < |\eta^\mu| < 2.4$

Figure 3: Muon identification efficiency obtained with T&P.

Single muon trigger eff

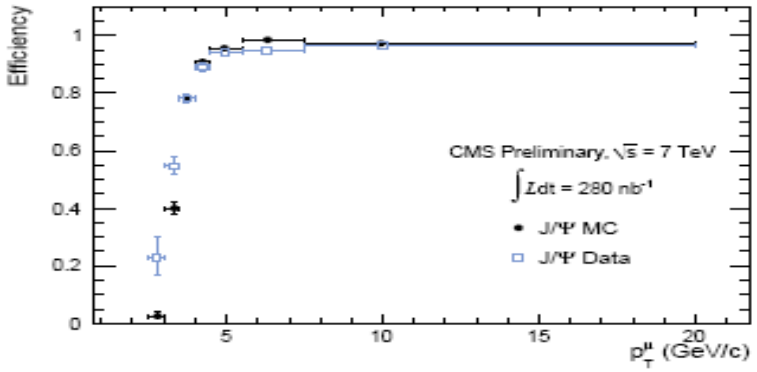

(a) Central region, $|\eta| < 1.2$

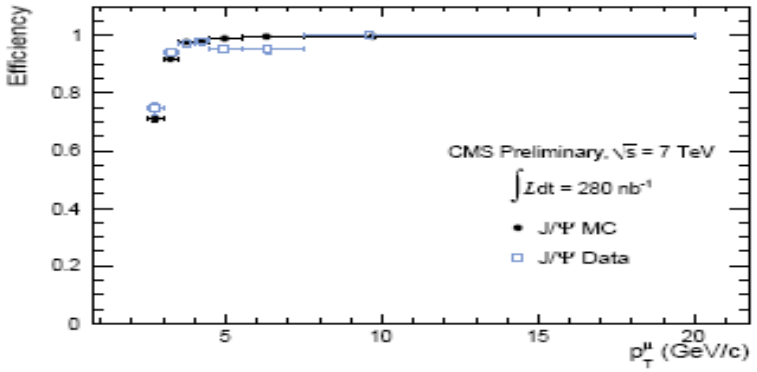

(b) Transition region, $1.2 < |\eta| < 1.6$

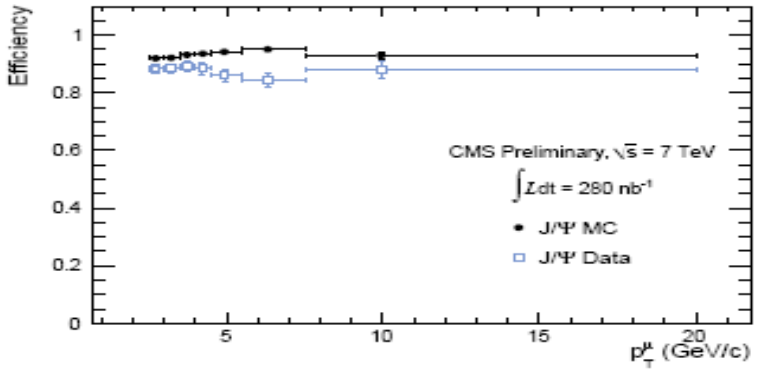

(c) Forward region, $1.6 < |\eta| < 2.4$

Figure 4: Single muon trigger efficiency, as a function of p_T^μ, evaluated with T&P.

Muon ID and trigger efficiencies

Table 2: Muon identification efficiencies from T&P; the uncertainties are statistical only.

p_T^μ(GeV/c) \ η^μ	(0.0, 1.2)	(1.2, 1.6)	(1.6, 2.4)
(2.5, 3.5)	-	-	$0.866 \pm^{0.050}_{0.046}$
(3.5, 4.5)	$0.884 \pm^{0.029}_{0.028}$	$0.960 \pm^{0.040}_{0.067}$	$0.910 \pm^{0.062}_{0.056}$
(4.5, 5.5)	$0.944 \pm^{0.033}_{0.033}$	$0.916 \pm^{0.059}_{0.056}$	$0.891 \pm^{0.075}_{0.068}$
(5.5, 7.5)	$0.919 \pm^{0.029}_{0.029}$	$0.807 \pm^{0.063}_{0.059}$	$0.864 \pm^{0.073}_{0.066}$
(7.5, 20.0)	$0.882 \pm^{0.037}_{0.036}$	$0.908 \pm^{0.092}_{0.088}$	$0.888 \pm^{0.112}_{0.099}$

Table 3: Muon trigger efficiencies from T&P; the uncertainties are statistical only.

p_T^μ(GeV/c) \ η^μ	(0.0, 1.2)	(1.2, 1.6)	(1.6, 2.4)
(2.5, 3.0)	-	-	$0.884 \pm^{0.013}_{0.014}$
(3.0, 3.5)	-	-	$0.885 \pm^{0.015}_{0.016}$
(3.5, 4.0)	$0.781 \pm^{0.017}_{0.018}$	$0.973 \pm^{0.009}_{0.011}$	$0.894 \pm^{0.017}_{0.019}$
(4.0, 4.5)	$0.890 \pm^{0.014}_{0.015}$	$0.981 \pm^{0.010}_{0.014}$	$0.885 \pm^{0.020}_{0.022}$
(4.5, 5.5)	$0.944 \pm^{0.009}_{0.010}$	$0.955 \pm^{0.012}_{0.014}$	$0.861 \pm^{0.020}_{0.021}$
(5.5, 7.5)	$0.948 \pm^{0.009}_{0.010}$	$0.954 \pm^{0.014}_{0.017}$	$0.846 \pm^{0.023}_{0.024}$
(7.5, 20.0)	$0.966 \pm^{0.009}_{0.011}$	$1.000 \pm^{0.000}_{0.017}$	$0.880 \pm^{0.028}_{0.033}$

Systematics J/psi yield

Table 2: Relative uncertainties (in percent) on the corrected yield, in each p_T bin: statistical , fina state radiation (FSR), p_T calibration, B-fraction, Non-prompt polarization, muon efficiency, ρ-factor, F functions

$p_T^{J/\psi}$ (GeV/c)	Statistics	FSR	p_T calibration	B-frac.	non-prompt polar.	Muon effic.	ρ	Fit function
				$\lvert y\rvert < 1.4$				
$4-6$	7.2	2.0	3.1	0.1	0.0	11.1	4.6	6.1
$6-8$	5.2	2.0	2.4	0.2	0.1	7.0	7.0	0.2
$8-10$	5.3	1.6	1.4	0.3	0.1	9.9	7.1	0.6
$10-30$	4.7	0.9	0.7	0.4	0.2	10.8	1.2	1.0
				$1.4 < \lvert y\rvert < 2.4$				
$0-1$	6.4	0.8	0.3	0.1	0.0	10.5	12.6	6.5
$1-1.5$	9.5	0.7	0.3	0.0	0.0	11.4	28.2	8.3
$1.5-2$	6.1	0.4	0.5	0.0	0.0	11.2	22.7	6.1
$2-3$	4.3	0.2	0.9	0.0	0.0	10.0	5.6	2.4
$3-4$	3.9	0.6	0.7	0.1	0.0	9.7	5.9	6.8
$4-6$	5.6	0.8	0.5	0.1	0.0	10.6	9.3	5.7
$6-8$	4.3	0.6	0.4	0.1	0.0	9.4	6.8	8.3
$8-10$	5.8	0.5	0.2	0.2	0.1	13.1	4.2	1.0
$10-30$	7.8	0.2	0.2	0.2	0.1	11.8	0.6	2.1

Systematics non-prompt J/psi yield

Table 5: Summary of relative systematic uncertainties in the b-fraction yield, in percent.

$p_T^{J/\psi}$ (GeV/c)	Misalign-ment	B-lifetime model	Vertex estimation	Background fit	Resolution model	Efficiency
			$\|y\| < 1.4$			
$4-6$	1.3	0.8	2.1	4.4	19.8	1.6
$6-10$	2.7	1.7	2.3	0.3	1.6	0.4
$10-30$	2.4	0.7	2.1	1.4	0.7	1.1
			$1.4 < \|y\| < 2.4$			
$0-2$	1.1	9.4	22.8	1.9	22.3	16.4
$2-4$	0.4	0.1	6.3	2.8	4.3	5.4
$4-6$	2.2	0.8	2.1	4.4	2.1	1.5
$6-10$	3.3	1.7	2.3	0.3	1.0	1.6
$10-30$	3.2	0.7	2.1	1.4	3.0	2.1

Systematics upsilon yield

Table 5: Relative values of the systematic uncertainties on the Υ(1S) integrated and differential production cross section times the dimuon branching fraction, assuming null production polarization, in units of percent. The momentum intervals are in units of GeV/c. The following abbreviations are used: Sp_{T}, T, T J/ψ and Σ, for the systematic uncertainties arising from imperfect knowledge of the momentum scale and resolution, T&P bias, residual bias from using the J/ψ resonance as a proxy for the Υ, and the sum in quadrature of systematic uncertainties. The uncertainty arising from imperfect knowledge of the production p_{T} spectrum is combined with Sp_{T}.

Δp_{T}	$\mathcal{A}^{\Upsilon}$	$\varepsilon_{\mathrm{muid}}$	$\varepsilon_{\mathrm{trig}}$	$\varepsilon_{\mathrm{trk}}$	FSR	$S\ p_{\mathrm{T}}$	T	TJ/ψ	PDF	Σ
0-2	0.5	9.5	3.4	0.6	3.5	0.2	2.1	2.0	0.4	11.1
2-3	0.5	10.0	3.5	0.6	4.1	0.6	2.1	1.4	0.4	11.7
3-5	0.6	10.0	0.5	0.6	3.7	0.5	2.0	1.3	0.4	11.0
5-8	0.6	11.0	6.2	0.6	3.2	0.6	1.8	2.0	0.4	13.3
8-12	0.6	10.3	6.5	0.6	2.6	0.8	2.2	2.9	0.4	13.1
12-20	0.4	13.3	14.0	0.7	2.3	1.6	2.2	4.3	0.4	20.1
0-20	0.6	10.4	5.1	0.6	3.4	0.5	2.0	2.0	0.4	12.5

Systematics open beauty

Table 3: Summary of systematic uncertainties. The systematic errors can vary depending on the muon transverse momentum and pseudorapidity as indicated by the range.

source	uncertainty
Trigger	3–5 %
Muon reconstruction	3 %
Tracking efficiency	2 %
Background template shape uncertainty	1–10 %
Background composition	3–6 %
Production mechanism	2–5 %
Fragmentation	1–4 %
Decay	3 %
MC statistics	1–4 %
Underlying Event	10 %
Luminosity	11 %
total	16–20 %

PV

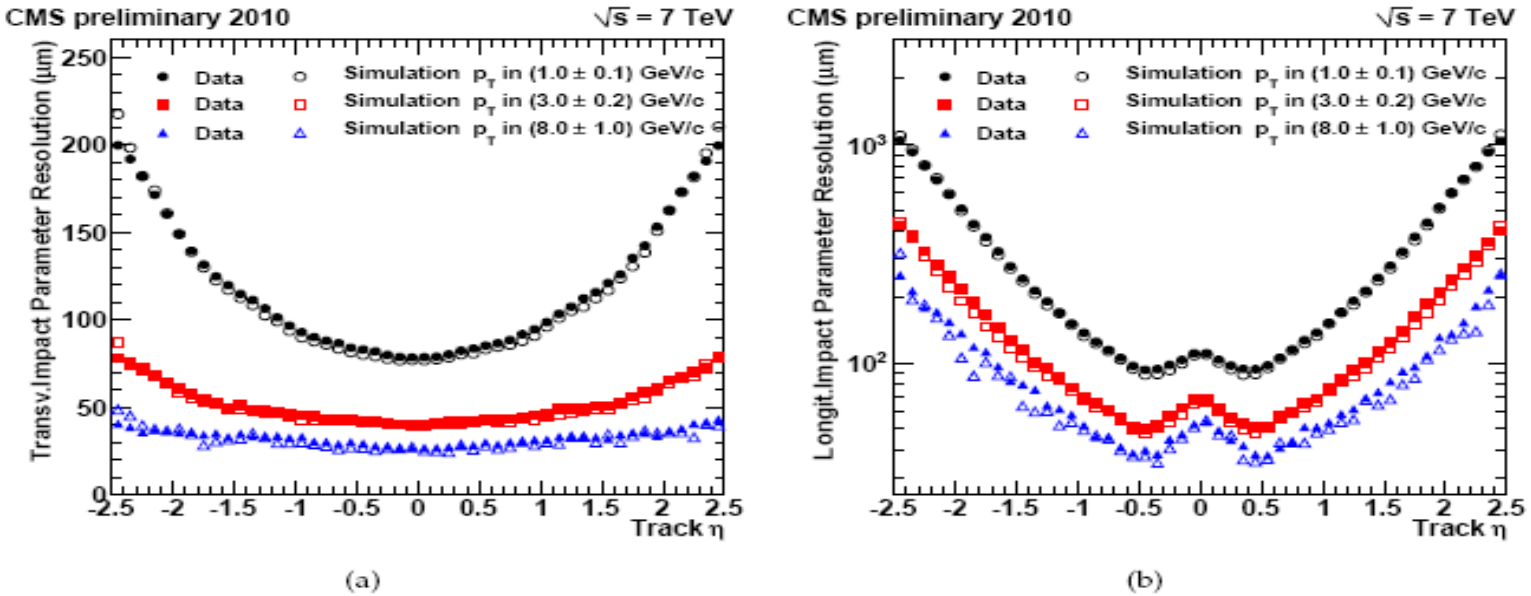

Figure 7: Measured resolution of the track transverse (a) and longitudinal (b) impact parameter as a function of the track η for transverse momenta in 1.0 ± 0.1 GeV/c (circles), in 3.0 ± 0.2 GeV/c (squares) and in 8.0 ± 1.0 GeV/c (triangles). Filled and open symbols correspond to results from data and simulation, respectively.

PV

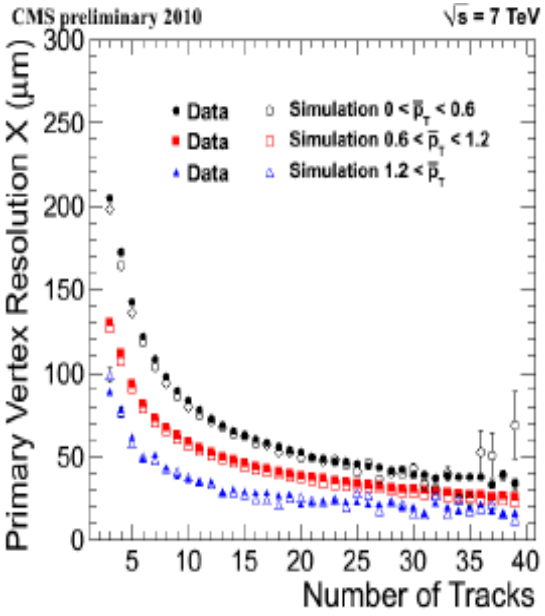
CMS preliminary 2010
√s = 7 TeV
Primary Vertex Resolution X (μm)
Number of Tracks
Data
Data
Data
Simulation 0 < p_T < 0.6
Simulation 0.6 < p_T < 1.2
Simulation 1.2 < p_T

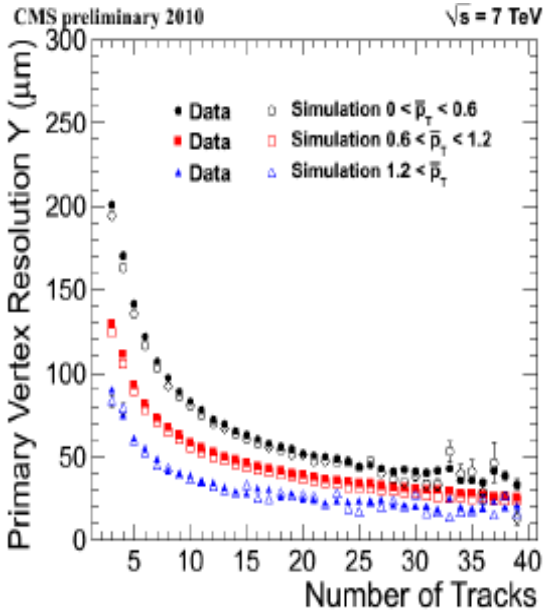
CMS preliminary 2010
√s = 7 TeV
Primary Vertex Resolution Y (μm)
Number of Tracks
Data
Data
Data
Simulation 0 < p_T < 0.6
Simulation 0.6 < p_T < 1.2
Simulation 1.2 < p_T

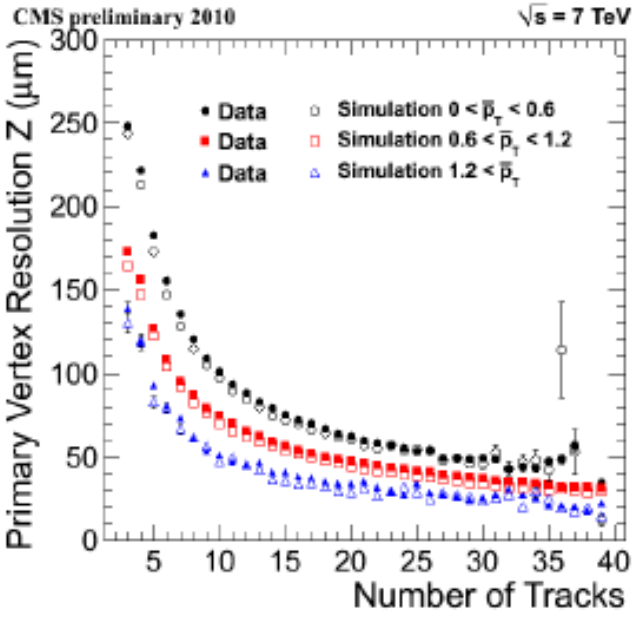
CMS preliminary 2010
√s = 7 TeV
Primary Vertex Resolution Z (μm)
Number of Tracks
Data
Data
Data
Simulation 0 < p_T < 0.6
Simulation 0.6 < p_T < 1.2
Simulation 1.2 < p_T

Material budget

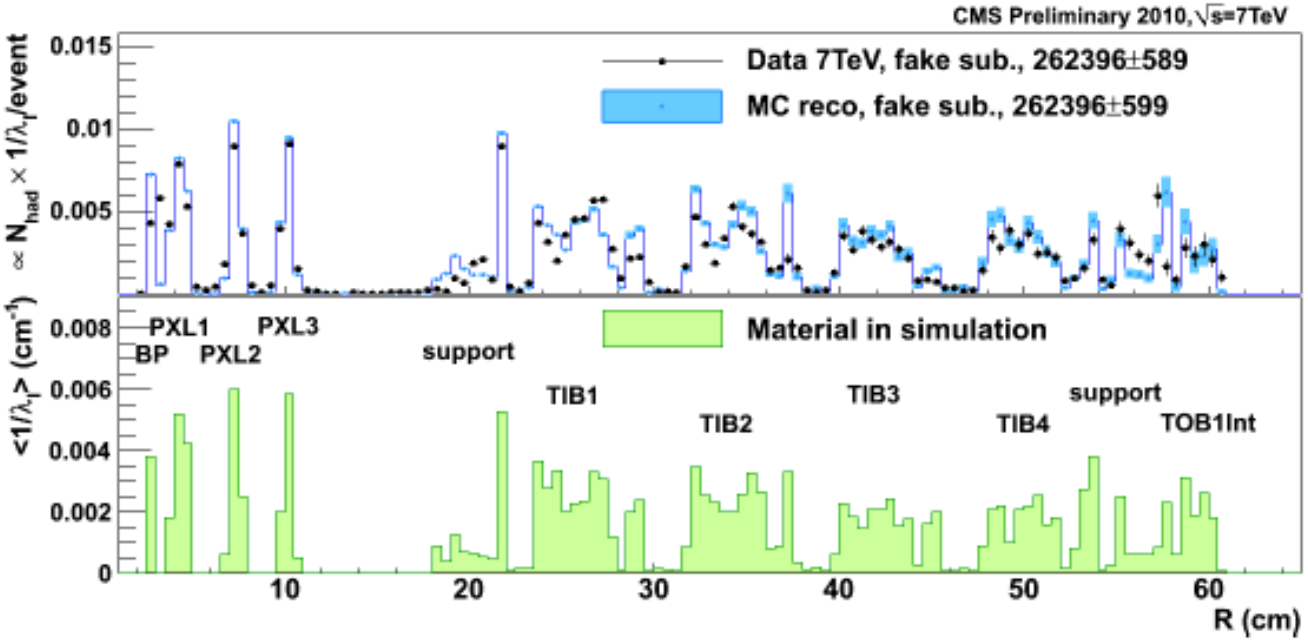

(b)

Figure 16: Material distribution versus the radius estimated from reconstructed photon conversions (a) and nuclear interactions (b). The radius is calculated with respect to the Pixel barrel detector centre. As a comparison, the histogram in the bottom panel represents the material distribution in the simulation in average X_0^{-1} per bin (a), and in average λ_I^{-1} per bin (b). In both plots the radius bin width is 0.5 cm.

Muon: fakes and efficiencies

Inclusive muons

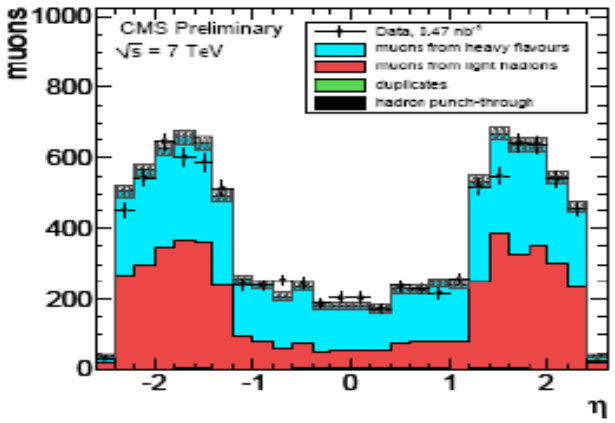

from $J/\psi \rightarrow \mu\mu$

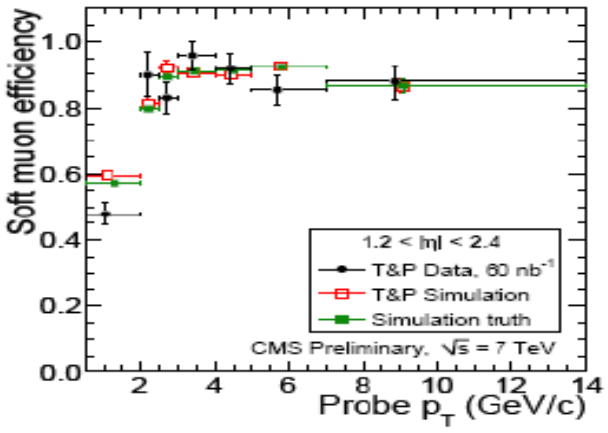

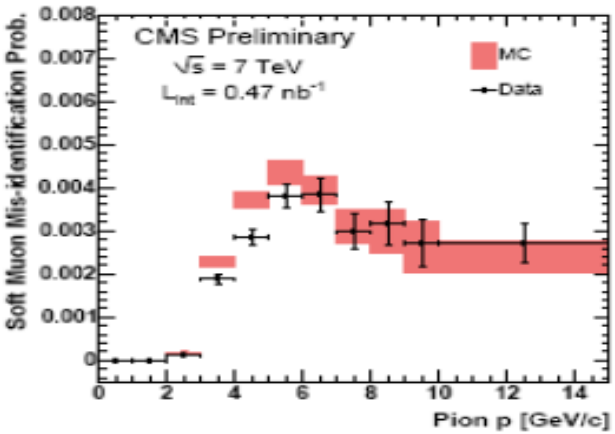

from $K^0_S \rightarrow \pi\pi$

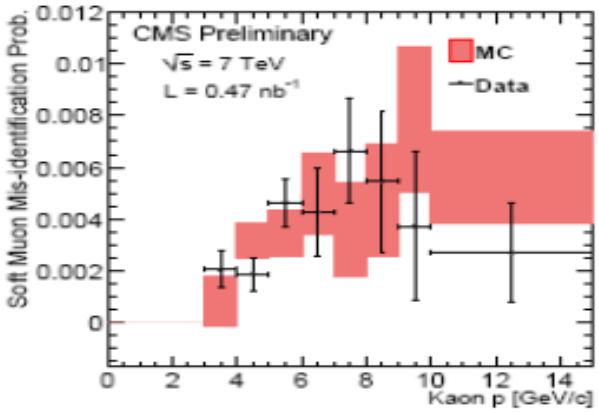

from $\phi \rightarrow KK$

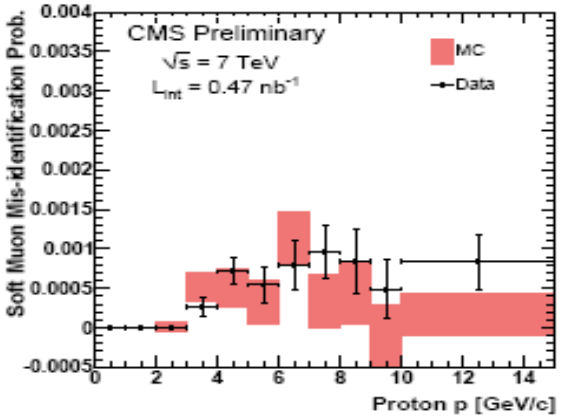

from $\Lambda \rightarrow p\pi$

Muons in jets

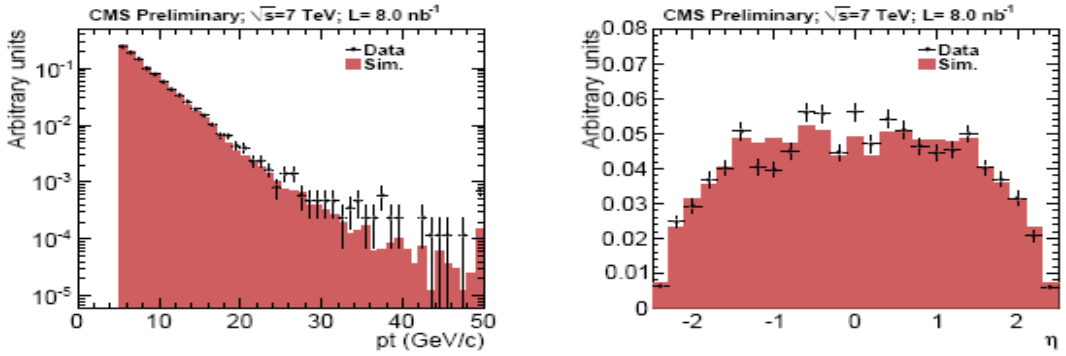

Figure 12: Distributions for muons associated with jets in data compared with MC in (left) p_T and (right) η. MC and data are normalized to unit area.

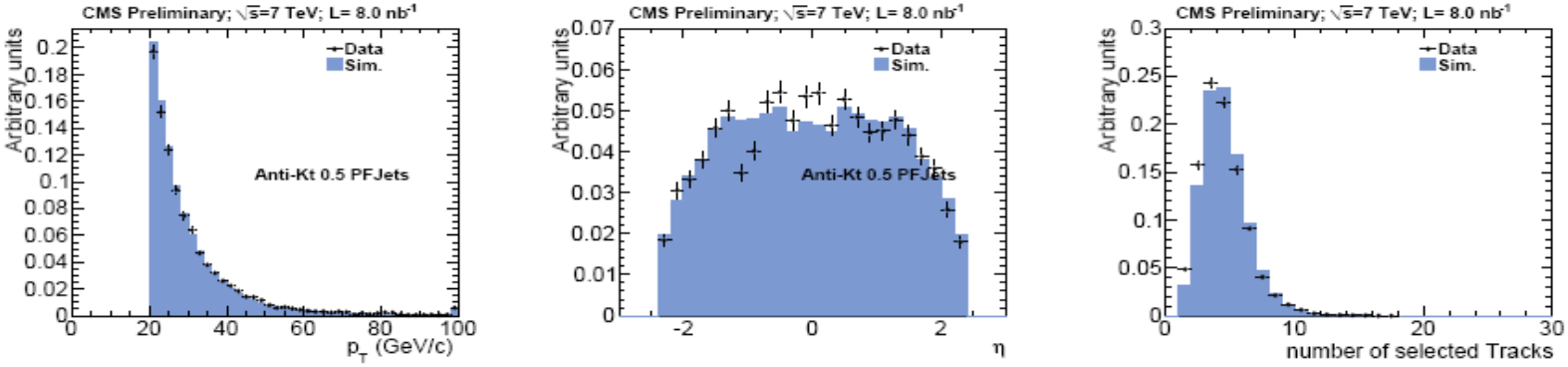

Figure 13: Distributions for muon jets in (left) p_T, (center) η and (right) number of tracks. MC and data spectra are normalized to unit area.

JEC

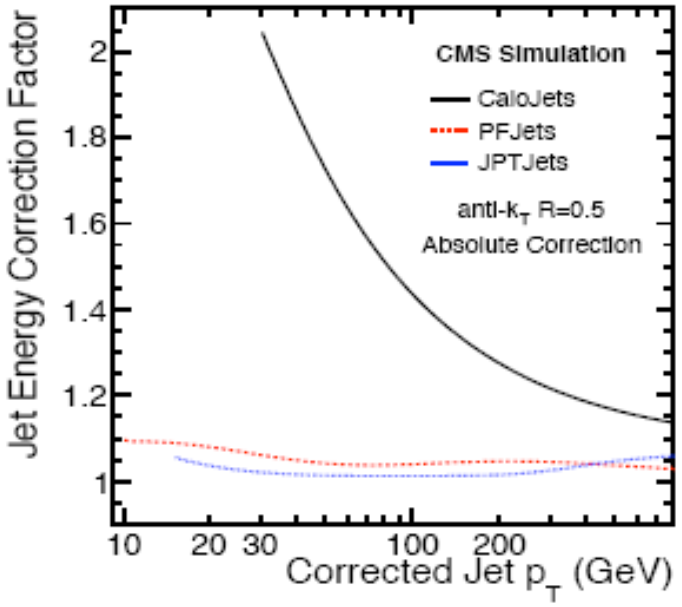

Figure 1: Absolute jet energy correction factors C_{Abs} derived from simulation for calorimeter, JPT, and PFlow jets at $\sqrt{s} = 7$ TeV as a function of corrected jet transverse momentum.